THERMAL MANAGEMENT METHOD FOR FOIL BEARINGS IN TURBINE HOT SECTION

by

TEJAS DEVIDAS PATIL

Presented to the Faculty of the Graduate School of

The University of Texas at Arlington in Partial Fulfillment

of the Requirements

for the Degree of

MASTER OF SCIENCE IN MECHANICAL ENGINEERING

THE UNIVERSITY OF TEXAS AT ARLINGTON

DECEMBER 2013

Copyright © by Tejas D Patil 2013

All Rights Reserved

Acknowledgements

I sincerely thank my committee chair, Dr. Daejong Kim for his guidance, and support throughout the course of research. I would also like to thank my committee members Dr. Kent Lawrence and Dr. Bo Wang.

I would like to express my gratitude to Kermit Beird and Sam Williams from machine shop for helping me at each stage in fabrication and assembly of test setup. I would like to thank my colleagues and friends in Microturbomachinary and Energy Systems Lab for their help and support. I would also like to acknowledge the financial support provided by Dr. Kim and sponsor.

And last but not the least, I would thank my family and friends for their love and support for all these years.

December 14, 2013

Abstract

THERMAL MANAGEMENT METHOD FOR FOIL BEARINGS IN TURBINE HOT SECTION

Tejas Devidas Patil, MS
The University of Texas at Arlington, 2013

Supervising Professor: Daejong Kim

Recently, Air Foil Bearings (AFB) are gaining higher industrial acceptance in micro-turbo machinery. AFB show high speed operating capability and environmental friendly operation in comparison to rolling element bearings. Utilization of ambient air as a lubricant eliminates maintenance of a pressurized oil lubricating system. AFBs are therefore a feasible alternative to oil lubricated bearings in small machines. High speed operation results in thermal management issues which can be solved through a suitable cooling mechanism. Axial cooling by passing air through bearing support structure (called bump foils) is the most commonly used. In this method, cooling is achieved in the heat exchange channels in corrugated foil structure.

A large thermal gradient exists on the journal shaft in the turbine hot section. Regardless of the cooling method, turbine hot section bearings have problem of maintaining uniform operating clearance along the axial direction due to uneven expansion of shaft along the shaft toward the turbine impeller.

This work presents an alternative method to reduce thermal gradient of bearing journal in turbine hot section by thermal isolation of the bearing journal from the main shaft. A high temperature test rig mimicking the turbine hot section was designed and the concept of thermal isolation of the bearing journal was implemented into the high temperature test rig.

Three-pad AFB was chosen for this experiment. The bearing journal was press fit on the main shaft but through a narrow ring adapter. The ring adapter reduces the contact surface area between the main shaft and journal; small contact area reduces direct heat transfer to the journal. Axial cooling was provided through the bump foil channels along the length of bearing by applying pressure drop across the bearing. Thermocouples measure temperatures of the bearing sleeve, bearing holder, ball bearing housing, heating cartridge, and support rolling element bearings in the rig pedestal.

Temperature distribution of stationary shaft along its length was recorded at stationary condition, and journal temperature was found to be substantially less than main shaft. Experiments were also carried out at cartridge heater temperature of 800^{o} C to reach steady operating condition at speeds up to 25krpm with a 45N load on the bearing.

Preliminary test results confirm that thermal isolation of the bearing journal is very effective and very uniform journal temperature could be achieved. The test should be further improved to achieve higher operating temperature and speeds.

Table of Contents

List of Illustrations

List of Tables

Chapter 1

Introduction

Gas film bearings are gaining popularity in micro-turbo machinery (shaft power less than 1MW and shaft diameters below 200mm) to achieve simple configurations as well as environmental protection and lower maintenance cycles by employing oil-free turbo machinery. With air used as lubricant, AFB can operate without thermal degradation of lubricant at high temperature and also at extremely low temperatures. Another advantage is increase in load capacity at high speeds while in typical rolling element bearing, load capacity reduces with speeds. Some common applications of AFB are micro turbines, air cycle machine, cryogenic turbo expander and auxiliary power unit.

1.1 Air Foil Bearings

Figure 1-1 shows a hydrodynamic single pad air foil bearing. Typical air foil bearings consist of three basic components; cylindrical sleeve, bump foil and top foil. The bump foil spot welded to the sleeve provides structural stiffness and coulomb (sliding) damping to the bearing. The sheet metal top foil is the actual bearing surface where hydrodynamic pressure is generated. Clearance exists between the top foil and rotor only when rotor is spinning. On the other hand frictional power losses are observed at time of start/stop, hence top foil is coated by a solid lubricant, for example: Teflon, aluminum bronze etc.

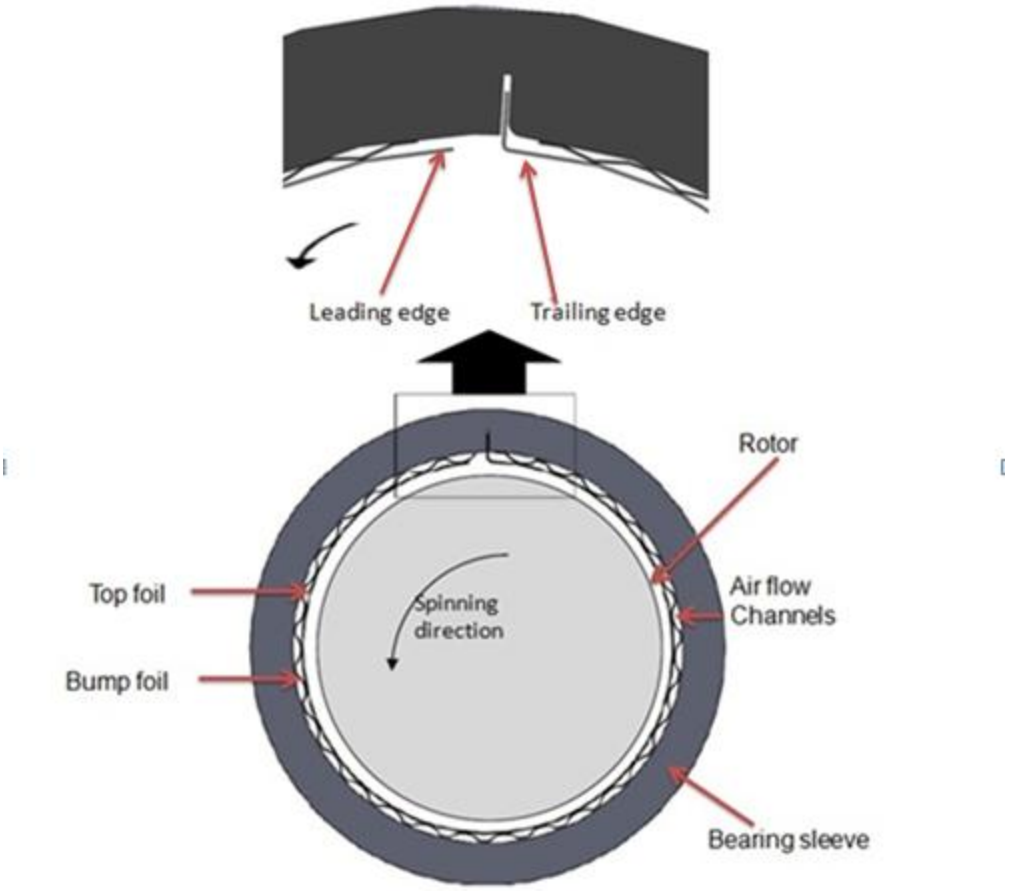

Figure 1-1 Typical air foil bearing

The foils are made of a Nickel-Chromium super alloy commonly known as Inconel. The bump and top foil are fixed at one end through spot welds to prevent movement. Direction of rotation is from leading edge (free end) to trailing edge (fixed end) as shown in Figure 1-1.

1.2 Principle of Operation

During normal operation there is no contact between the rotating journal shaft and bearing surface. Bearing clearance is maintained through hydro-dynamic pressure built up by two mechanisms: Wedge effect and squeeze film effect. Converging wedges are formed between the stationary bearing sleeve and a rotating journal with an eccentricity as shown in Figure 1-2. Pressure built up in these wedges is termed as wedge effect. When the air film in clearance is squeezed, molecules try to escape but surrounding molecules in the air film resist this escape, thus build up a positive pressure termed as squeeze film effect. Both effects help the shaft to reach a lift off speed and eventually the shaft becomes airborne so that nearly friction free operation is achieved.

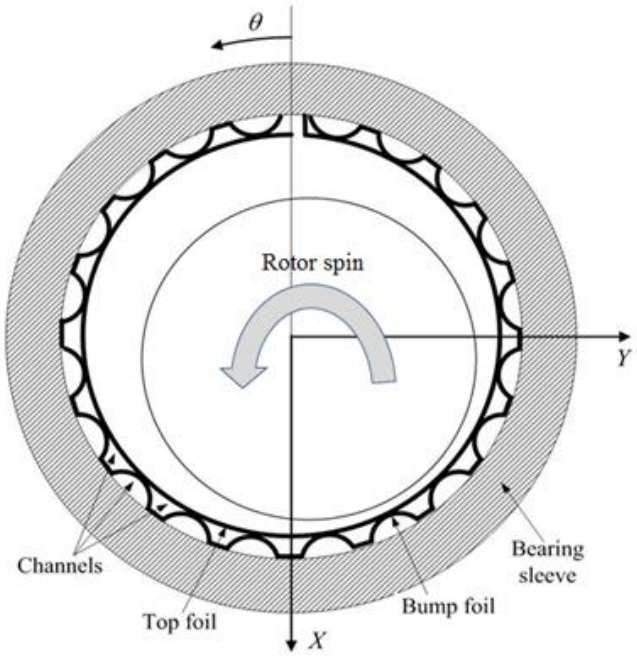

Figure 1-2 Foil bearing in normal operating condition, adopted from ref [1]

1.3 Multi-Pad Air Foil Bearing

Single pad air foil bearings with uniform clearance along the circumferential direction have higher load capacity than multi pad bearings, but they suffer lower onset speed of instability. The uniform bearing clearance leads to dynamic instability at high speeds because of large cross coupled stiffness. To avoid this instability bearing configuration with non-uniform clearance is often adopted.

Figure 1-3 shows the location of minimum set bore film thickness in the pad (θ_{SB}) and pad angular width (θ_{pad}). Offset ratio given by equation (1.1) is the ratio of these angles. Non-dimensional preload (r_p) is ratio of distance between the rotor center and the pad center (Figure 1-4) to nominal clearance given by equation (1.2). Offset ratio and hydrodynamic preload are crucial bearing design parameters. Added advantage of multi pad bearings is the ability to support load in multiple directions

$$\gamma = \frac{\theta_{SB}}{\theta_{pad}} \tag{1.1}$$

$$r_p = \frac{d}{C} \tag{1.2}$$

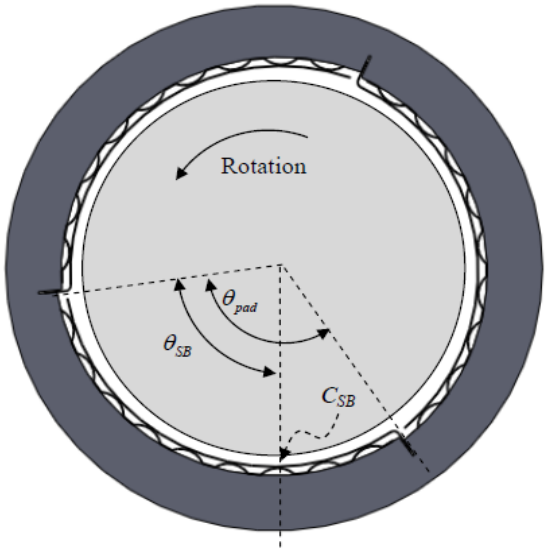

Figure 1-3 Offset preloaded three pad AFB

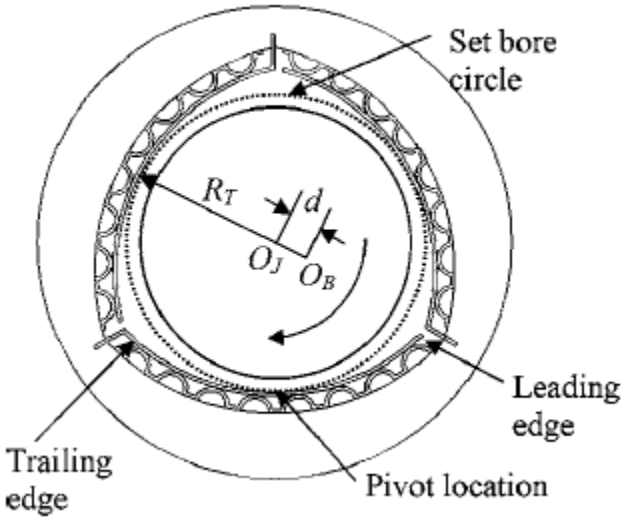

Figure 1-4 Preload in three pad foil bearing, adopted from ref [2]

1.4 Disadvantages

AFBs suffer from lower load carrying capacity at low speeds and instability due to cross coupled stiffness at high speeds. Thermal management issue at high speeds and friction/wear during start/stop are also disadvantages.

Thermal runaway is a major issue due to rotor centrifugal and thermal expansion. Expansion of rotor lead to reduction in film thickness leading to increase in journal temperature and expansion due to viscous shearing (of gas film) to the point of bearing seizure. Hence rotor expansion limits load capacity and maximum speed of operation.

Chapter 2

Literature Review

Salehi et al [3] studied thermal characteristics of foil bearings using analytical method and compared their calculation with experimental data. They evaluated temperature distribution in air film by using Couette approximation to energy equation in association with Reynolds equation. Results obtained from analysis were compared to experiments performed on foil bearing with diameter of 100mm under variable load (50-350 lbf) at 30krpm. They found a difference of approximately 19% between the analytical results and experimental data. They concluded Couette approximation to be a considerable tool for analytical method. In addition they confirmed majority of heat exchange between cooling air and air film is through conduction over top foil.

Radil and Howard [4] at NASA, examined effect of change in radial clearance on load carrying capacity of AFB. Experiments were performed using two foil bearings with 35mm nominal diameter and operating at maximum speed of 30krpm.Variable radial clearance was obtained by reducing journal diameter. The results demonstrate foil bearings have an optimum clearance to attain maximum load capacity. They concluded there are two regimes relative to this optimum clearance. When clearance lower than optimum is chosen the bearing exhibits better load capacity coefficients but is inclined to thermal run away and eventual failure. When operating at clearance higher than optimum, the bearing shows a very small drop (approximately 20%) in load capacity but is free from thermal issues. The effects on performance parameters like structural stiffness and damping were not discussed.

At Army Research Lab, Radil and Zeszotek [5] performed multiple experiments to determine the temperature distribution in air film for a variety of speeds and loads. Thermal gradient along axial and circumferential direction were analyzed. Location of thermocouples was selected on backside of bump as shown in Figure 2-1 Experiments were carried out for variable speeds (20krpm-50krpm) and loads (9-222 N). They concluded increase in speed and load both lead to rise in bearing temperature. Also it was observed maximum temperature occurred at center of bearing and not edges.

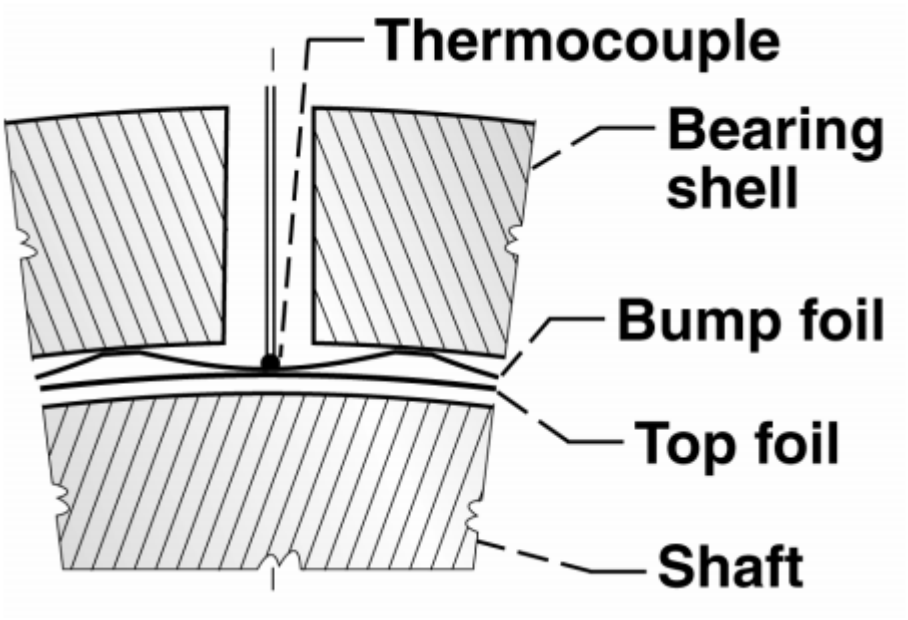

Figure 2-1 Location of thermocouple on backside of bump foil to monitor temperature of bearing, adopted from ref [5]

Dykas and Howard [6] determined cause of shaft failure operating at high temperature and speed through experiments and finite element analysis. Cause of failure was described as increase in shaft diameter leading to rubbing at high speed and eventually system failure. Increase in shaft diameter was mainly due to circumferential

loading of corrected imbalance weight and thermal gradient along axial direction. To avoid failure they have suggested the following preventive techniques

- Increasing journal thickness to reduce thermal gradient by increasing heat conductivity in axial direction.
- Providing tight manufacturing tolerances.
- Providing a cooling mechanism to journal at center of bearing to reduce overall temperature.

Radil et al [7] checked three different cooling methods. They are direct method, indirect method and axial cooling. In direct cooling method, air is impinged directly on inner surface of rotating hollow journal shaft. For indirect method, cooling air was blown inside hollow journal shaft to mimic axial flow inside cylindrical cavity. In axial cooling method, cooling air is passed through channels formed by bump foil. Furnace heats the experimental section up to 260^{o} at 1 atm pressure. 222N was applied to the test section, and all methods were evaluated for flow rates of 0.06, 0.11, and 0.17 m^3/min at 200^{o}C. Effectiveness of the three cooling methods was evaluated by measuring bulk bearing temperature and thermal gradient along axial direction. Traditional axial cooling was concluded to be a better cooling technique over direct and indirect methods.

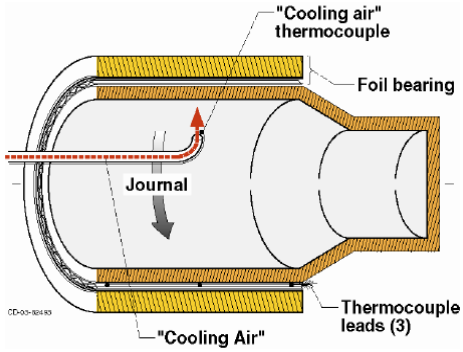

(a) Direct method

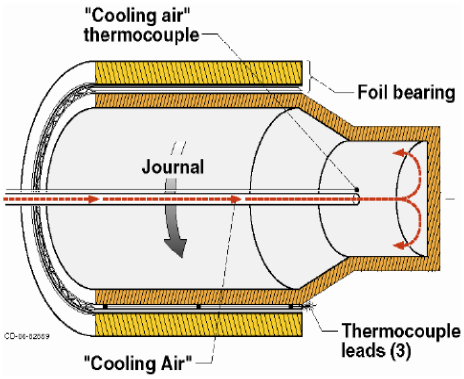

(b) Indirect method

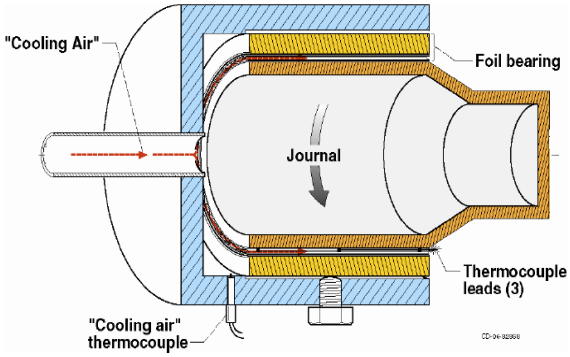

(c) Axial cooling method

Figure 2-2 Different cooling methods evaluated (a) Direct method (b) Indirect method (c) Axial cooling method, adopted from ref [7]

Kim T. and San Andres [8] at Texas A&M University conducted experiments to verify effect of increasing temperatures on structural stiffness of foil bearings while the shaft is stationary with diameter of 38.17. It was mounted on a hollow stationary shaft heated to a high temperature (188^{o}C) by inserting a cartridge heater into hollow cavity (Figure 2-3). Radial clearance increased due to higher expansion of bearings housing compared to shaft. Thus for a steady load (133N) a decrease in stiffness was observed. With increased excitation frequencies (20 to 400 Hz) increase in dynamic stiffness was observed. Increased shaft temperature also caused a decrease in viscous damping of bearings.

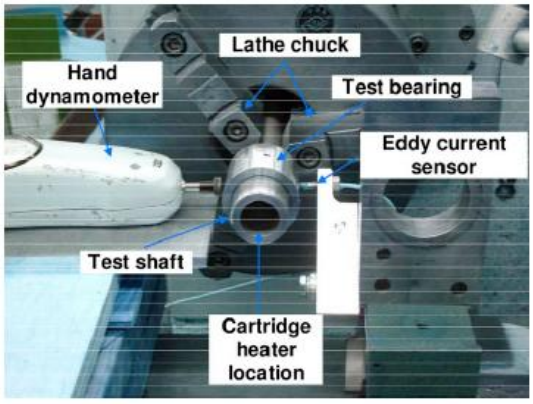

Figure 2-3 Test setup to evaluate structural stiffness with steady loading, adopted from ref [8]

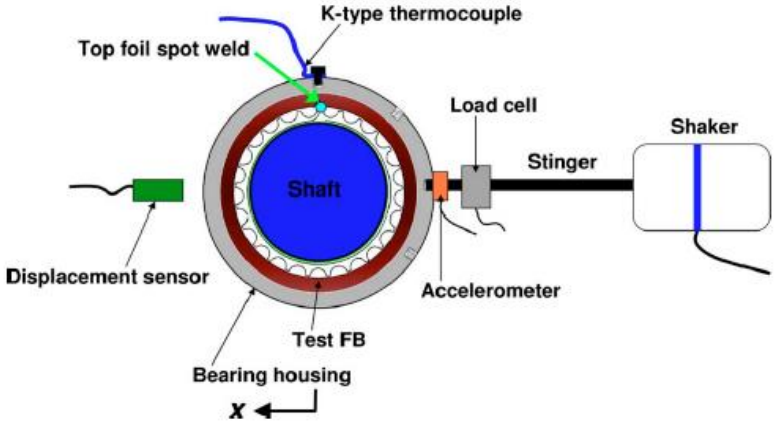

Figure 2-4 Test setup to evaluate stiffness by dynamic load excitation, adopted from ref [8]

Radill and Batcho [9] tested a different cooling method by introducing cooling air injection on the shaft inside the bearing. They found three major issues in general foil bearing thermal management;

1. Effect of localized temperature rise on elasticity of bump foil.
2. Journal thermal runaway leading to bearing failure.
3. Thermal gradient along axial direction of journal shaft.

Cooling technique they used involved forcing the cooling air directly into hot air film of single pad foil bearing. The air was impinged through a hole through sleeve into discontinuity region of top foil (the gap between the leading edge and trailing edge, shown in Figure 2-5). Experiments were performed at high speed (20krpm-50krpm) supporting a load of 222N .Two flow rates 0.017 kg/min and 0.051 kg/min were tested. Higher flow rate demonstrated better effectiveness in reducing thermal gradient and overall bearing temperature. They concluded this method was less effective than traditional axial cooling method. Moreover, it was unclear whether cooling was obtained

due to mixing of cooling air in fluid film or replacement of the retained slug of hot air with fresh cooling air.

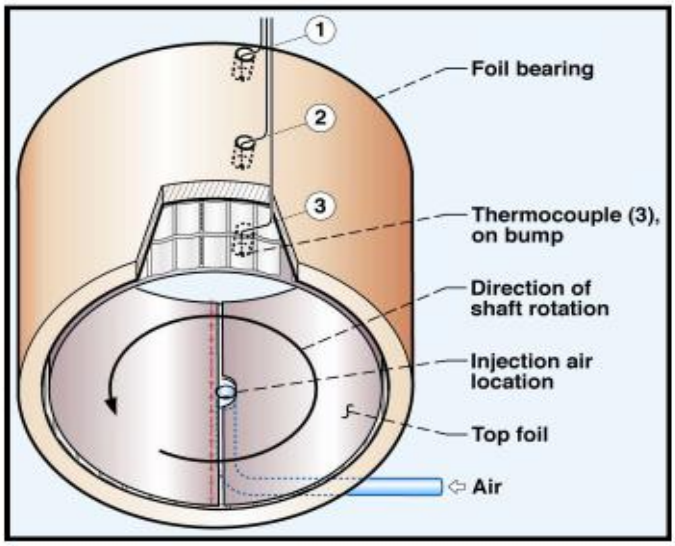

(a) Location of hole for air injection

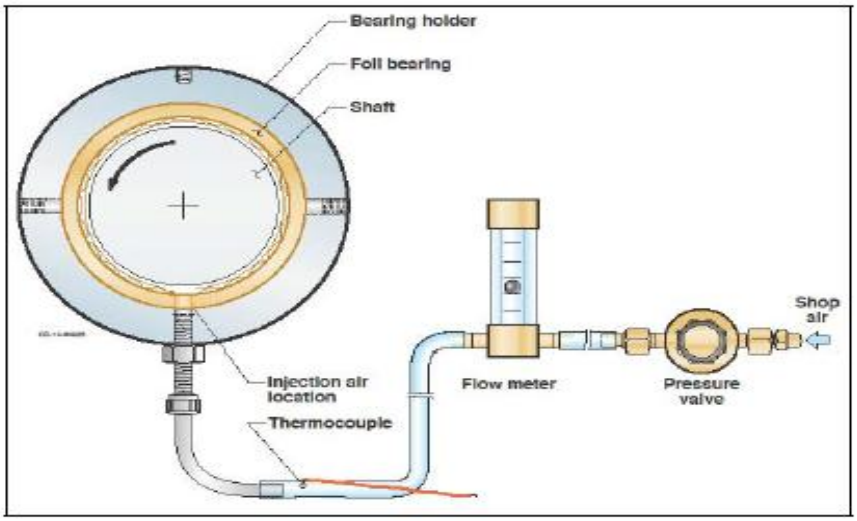

(b) Test set up

Figure 2-5 Cooling technique by injecting cooling air directly into air film of AFB

(a) Location of holes for air injection (b) Test set up, adopted from ref[9]

Kim and Lee [1] developed a 3-D thermo-hydrodynamic model of AFB by applying axial cooling through structure. Temperature of air film, top foil, bump foil, bearing sleeve, and shaft could be calculated when cooling air pressure is introduced.. Effective heat transfer resistance between top foil and bearing sleeve were implemented to analysis. The cooling channels create thermal subsystems due to corrugated structure of bump foil. The heat transfer through these sub systems is shown in Figure 2-6.The bump foil channels were modeled as primary and secondary channels. It was observed that heat transferred to secondary channel was from bump foil and not top foil. Primary channels were concluded to be more effective in cooling compared to secondary channels. They also concluded foil thermal expansion contributes to 1% decrease in clearance while journal growth contributes to 20% decrease. Thus rotor growth (thermal or centrifugal) is main cause of thermal runaway.

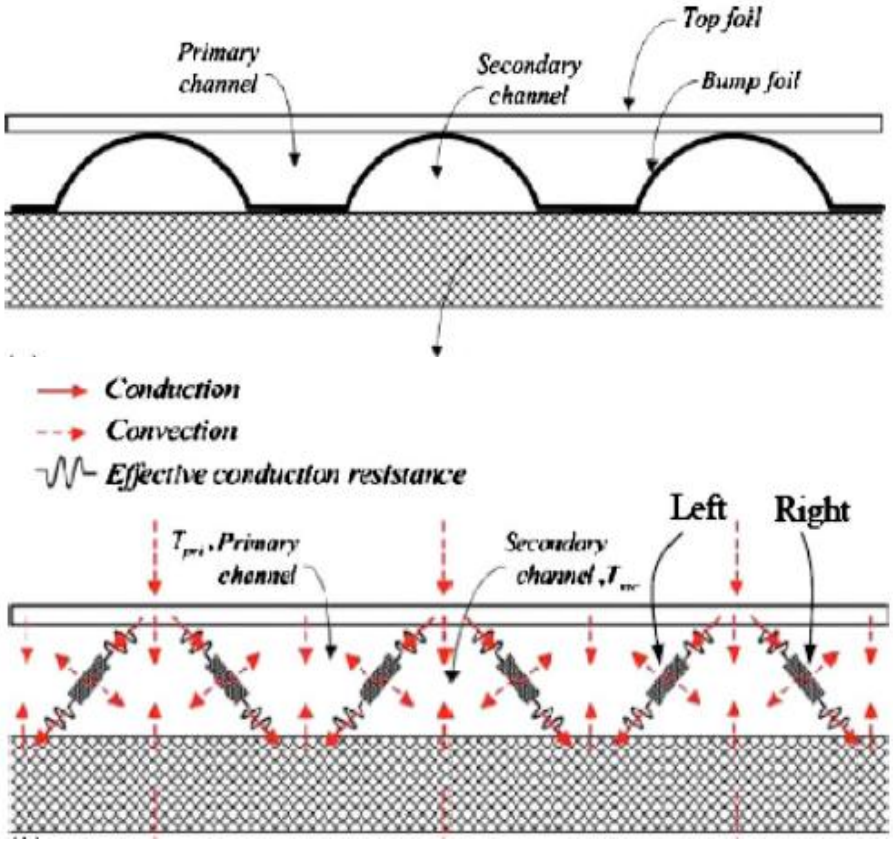

Figure 2-6 A plate fin type heat exchanger model of bump foil structure, adopted from ref [1]

Kim and Ki [10] extended the three dimensional thermo-hydrodynamic (3D THD) model mentioned in [1] to a turbine simulator hardware designed to mimic 50kW gas turbine. The turbine simulator could mimic equivalent thermal conditions and axial thrust loads similar to the actual 50 KW gas turbine. This extended model could calculate temperatures of cooling air plenums (the cavities to/from cooling air are introduced and discharged, and they are formed on both side of the bearing), bearing sleeve, housing and rotor exposed to the plenums. Computational fluid dynamic model of region where cooling air enters the film near the leading edge of top foil was adopted to estimate better

inlet thermal boundary conditions. Model was analyzed at 50krpm with cooling air pressure of 4000 Pa for traditional axial cooling through bump channels and rotor cooling through channels formed on the rotor as shown in Figure 2-7.

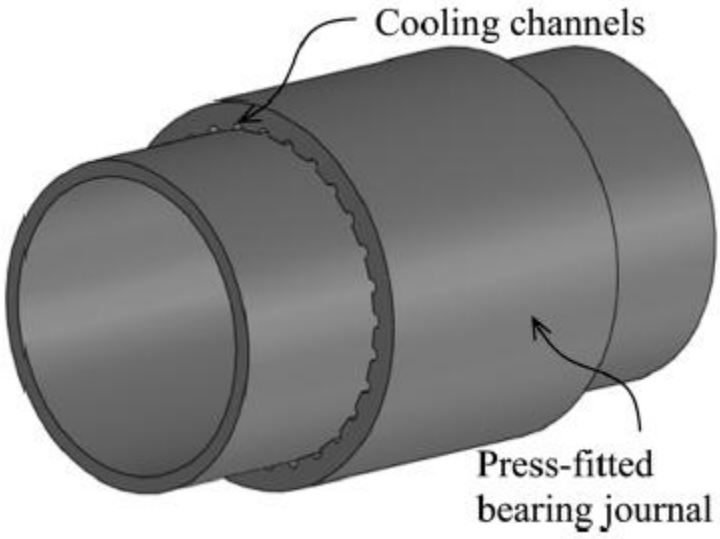

Figure 2-7 Rotor design with cooling channels, reference from [10]

Kim et al [11] compared axial cooling method with radial injection method. Thermal management is a major issue during operation of AFB at high speeds. Three dimensional energy equations and Reynolds equation are used to evaluate temperature distribution in the air film and all bearing components. Temperature field of AFB could be solved by knowing thermal boundary conditions at leading edge. Mass and energy balance equations were applied to leading edge groove (Figure 2-8) to determine boundary conditions;

$$\dot{m}_{mixing} = \dot{m}_{inlet-\lambda}\ \dot{m}_{exit} \quad \text{where } 0 << \lambda < 1 \tag{2.1}$$

$$T_{inlet} = \frac{\lambda \dot{m}_{exit}\, c_p \left(T_{exit}\right) T_{exit} + \dot{m}_{mixing}\, c_p \left(T_{mixing}\right) T_{mixing}}{\dot{m}_{inlet}\, c_p T_{inlet}} \qquad (2.2)$$

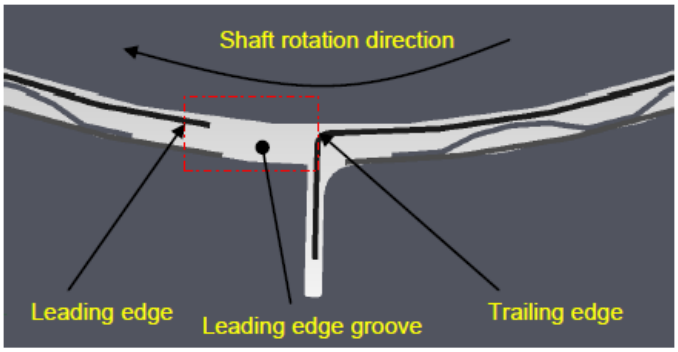

Figure 2-8 Leading edge region at top foil discontinuity where mixing of cooling air occurs, adopted from ref [11]

λ is defined as fraction of exit flow attached to rotor surface and re-circulated to next leading edge also known as recirculation ratio [10]. $\dot{m}_{mixing}$ corresponds to cooling air mixed in leading edge and T_{mixing} is temperature of leading edge groove. The ideal case (λ=0) of $T_{inlet}=T_{mixing}$ is the most effective [12], but infeasible as it requires complete breakdown of thermal boundary layer at leading edge. Kim et al [11] studied effect of radial injection cooling by impinging cooling air directly onto the rotating journal shaft. This method is the most practical approach to match ideal case. Also for low pressure drop and high rotor speed mixing of cooling air near leading edge decreases. They concluded both axial cooling method and radial injection method are equally effective in controlling bearing overall temperature at low flow rates but radial injection cooling has better temperature control on the shaft.

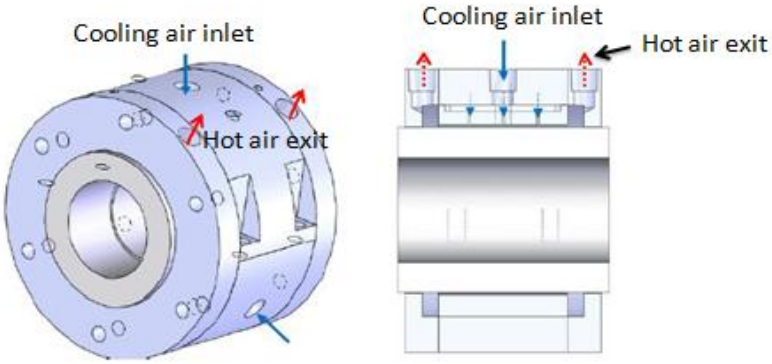

(a) Air flow direction in radial cooling

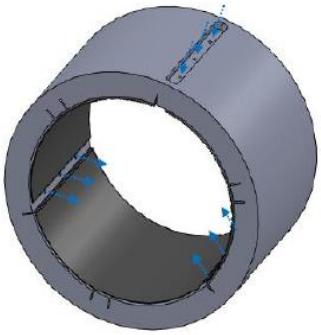

(b) AFB with radial injection holes at the leading edge region

Figure 2-9 Modified bearing holder and sleeve for radial injection, adopted from ref [11]

Chapter 3

Purpose of Experiment

3.1 Problem Statement

The temperature at the turbine end is always higher than the compressors end in any gas turbine configuration. During normal operation there is non-uniform expansion of shaft in axial direction forming a taper as shown in Figure 3-1.

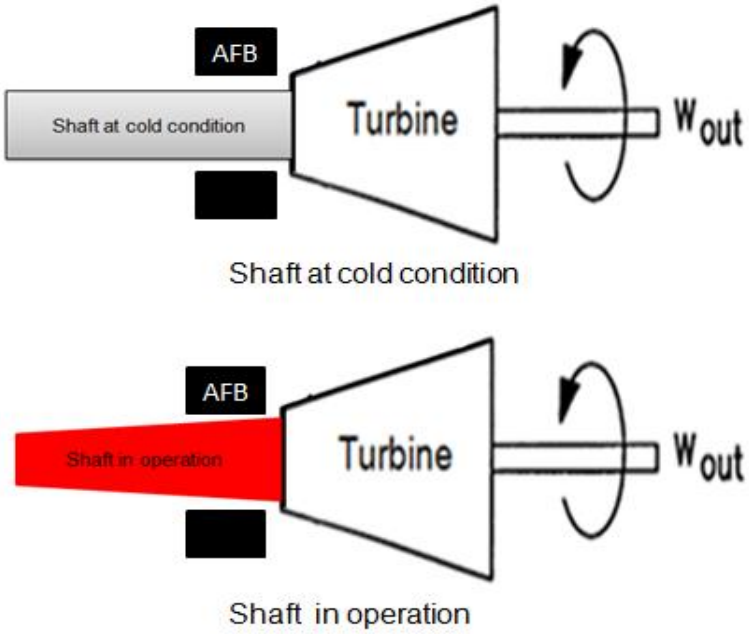

Figure 3-1 Taper formation due to non-uniform expansion of shaft at turbine hot section

Optimum clearance selected for ambient temperature application is easily eaten up at one side of the bearing by uneven shaft thermal expansion at the turbine hot section. Hence, to accommodate this uneven expansion, initial bearing assembly clearance is large. Further, to match this large radial clearance, the blade tip clearance of impellers has to be sufficiently high.

Blade tip clearance is an important design consideration. The gap is designed to avoid rubbing between blades and housing. Losses already exist due to this gap commonly known as ‘tip leakage loss’ which arises due to a leakage flow. Therefore, larger the gap higher the leakage flow leading to loss in power and efficiency of turbine, thus affecting the primary function of the gas turbine. Operating at an optimum tip clearance is extremely important to obtain maximum efficiency and power.

Thus, too large bearing clearance to accommodate the uneven shaft thermal expansion causes adverse effect on the system efficiency, offsetting benefit of reduced windage loss from the foil bearings.

This issue could be solved by controlling the thermal expansion of the journal shaft over the bearing area and reducing the thermal gradient to maintain uniform clearance along the axial direction.

Traditional axial cooling is the simplest cooling technique in practice to control the overall bearing temperature. The axial cooling uses secondary leakage flow through seals of compressor and turbines. Thus cooling air flow naturally exists because of pressure drop from compressor to turbine. The cooling air is discharged to turbine without any hardware modification (Figure 3-2).

The radial injection method used in ref [11] is alternative method for better controlling the shaft temperature and thermal gradient, Even if the radial injection cooling reduces the thermal gradients of the shaft, it does not solve the large thermal gradient problem originated from proximity of the bearing from the turbine impeller. Even if the locations radial injection holes can be tailored (more toward turbine) to reduce the large thermal gradients to some extents, requirement of very good seals and air delivery/discharge systems add complexity to the system (Figure 3-3).

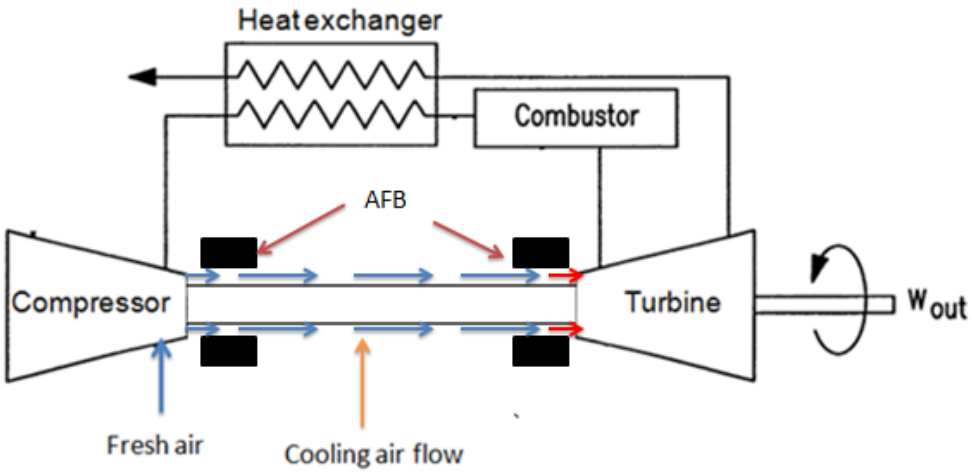

Figure 3-2 Flow of cooling air in axial cooling method for actual gas turbines

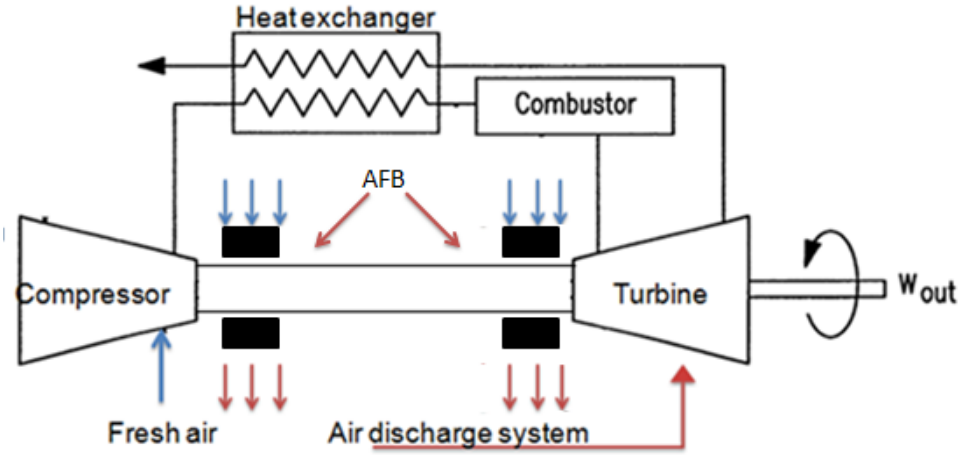

Figure 3-3 Flow of cooling air in radial injection cooling for gas turbines

3.2 Research Objective

The first objective of this thesis is to design a new bearing journal configuration at the turbine hot section that allows the commonly used axial cooling and also eliminates the large thermal gradient. The second objective of this research is design and commissioning of a test rig to mimic turbine hot section with the new journal shaft configuration. The high temperature test rig must be capable of operating above 500^{o}C.

Chapter 4

Experimental Setup

This chapter presents the details of experimental setup designed to mimic turbine hot section. The hardware used to perform the test and data acquisition is discussed in this section. The Figure 4-1 shows the CAD model of the test rig setup.

1. Electric motor
2. Pedestal housing with ball bearing
3. Test foil bearing inside the holder
4. Heating cartridges
5. Torque measuring device
6. Loading mechanism

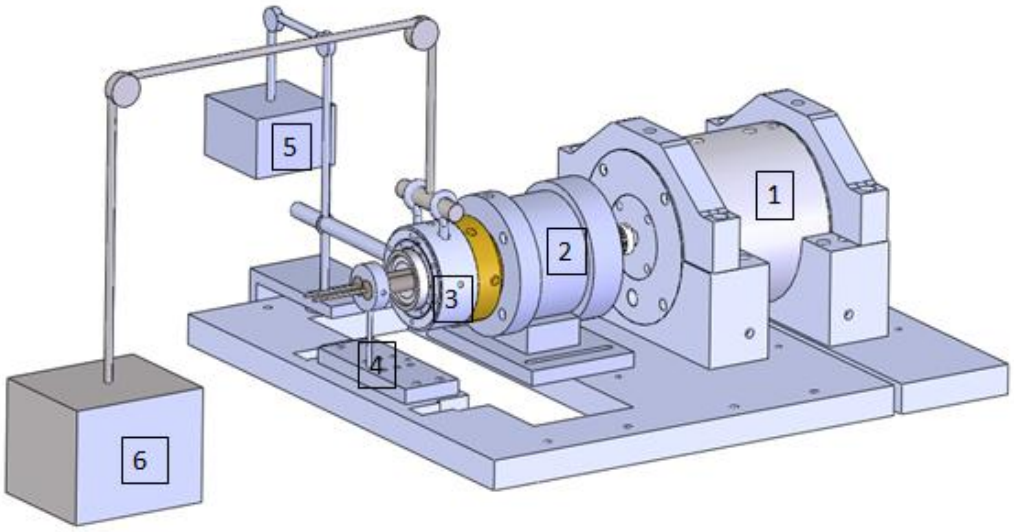

Figure 4-1 CAD model of test rig to mimic turbine hot section

4.1 Test Rig Configuration

Test rig can be split into three main sections; (1) The 10 KW motor used by [11] was employed for high torque requirement. (2) The pedestal with rolling element bearings to support the shaft and bearing journal. (3) The test section comprises of heating

cartridges, torque measuring mechanism and loading mechanism for AFB. The motor drives the entire system through a flexible coupling as shown in Figure 4-2.

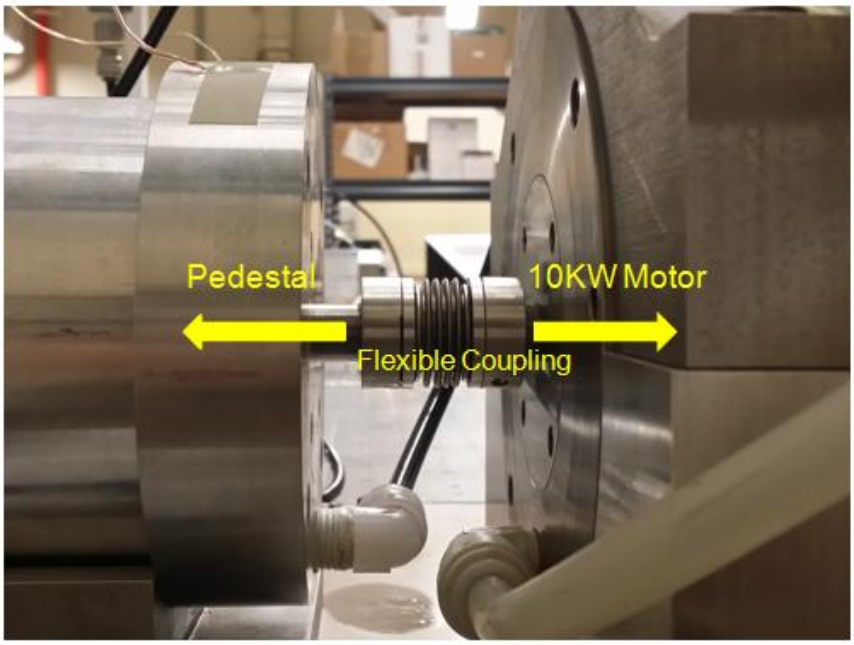

Figure 4-2 Flexible coupling used to drive system

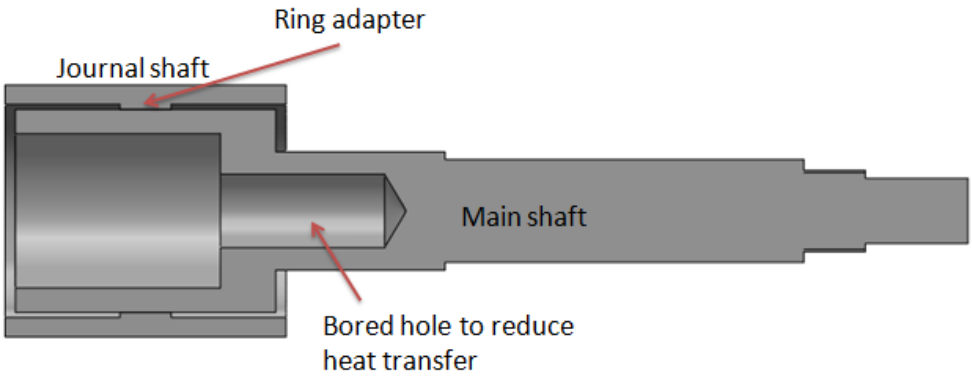

Figure 4-3 Journal isolation from main shaft using a ring adapter

The bearing journal shaft was thermal isolated from the main shaft by adopting a narrow ring embossed on the journal inner diameter. Bearing journal was press-fitted on the ring adaptor. The ring adapter reduces heat transfer from the main shaft to the journal

and also the location of the ring adaptor allows spreading of thermal energy to the bearing journal evenly regardless of the heater location. Also shown in Figure 4-3, the main shaft is hollow to mimic actual hardware encountered in small gas turbines. Also material was removed from shaft body to reduce heat transfer to ball bearings.

4.1.1 Rotordynamic Analysis

Rotordynamic analysis was performed using commercial software (XL ROTOR). The shaft was modeled as multiple beams between different stations as shown in Figure 4-4. The stations and beam were defined using Table 4-1.

Table 4-1 Beam and station definition input table

1	INPUT TABLE OF BEAM AND STATION DEFINITIONS, MORE THAN ONE BEAM PER STATION IS OK										
2	Station	Length	OD	ID	Density	Elastic Modulus	Shear Modulus	Added Weight	Added Ip	Added It	Speed Factor
3	#	mm	mm	mm	kg/m^3	N/m^2	N/m^2	kg	kg-m^2	kg-m^2	
6	1	20	12.7	0	7800	2.00E+11	7.70E+10	0	0	0	1.0
7	2	12	15.88	0	7800	2.00E+11	7.70E+10	0	0	0	1.0
8	3	6	20	0	7800	2.00E+11	7.70E+10	0	0	0	1.0
9	4	58	20	0	7800	2.00E+11	7.70E+10	0	0	0	1.0
10	5	6	20	0	7800	2.00E+11	7.70E+10	0	0	0	1.0
11	6	9.65	23	0	7800	2.00E+11	7.70E+10	0	0	0	1.0
12	7	25.49	23	14.28	7800	2.00E+11	7.70E+10	0	0	0	1.0
13	8	10.8	39.46	14.28	7800	2.00E+11	7.70E+10	0	0	0	1.0
14	9	14.6	39.46	30	7800	2.00E+11	7.70E+10	0	0	0	1.0
15	10	25.4	39.46	30	7800	2.00E+11	7.70E+10	0.23889	0	0	1.0
16	11	0	0	0	0	0	0	0	0	0	1

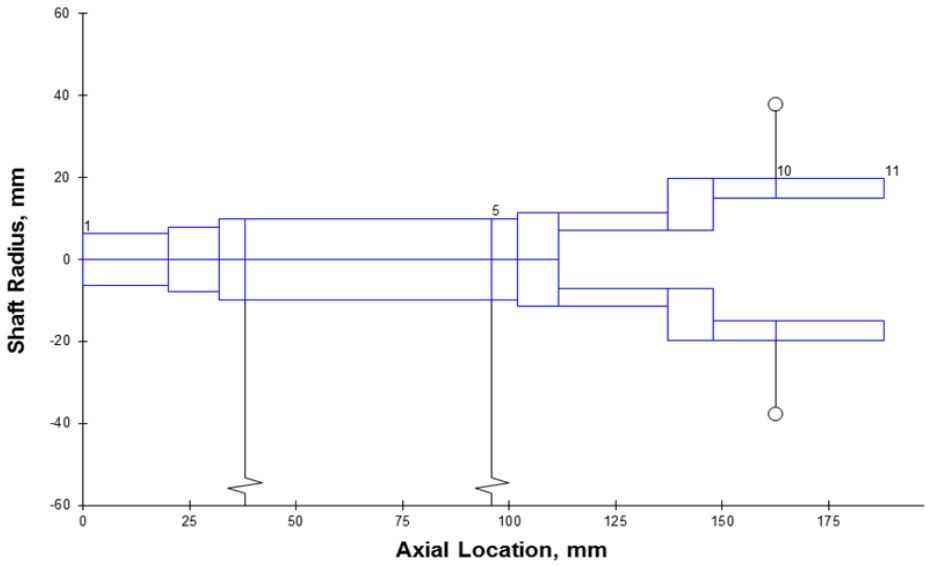

Figure 4-4 Rotor modeled as series of beams between 11 stations

Critical speed is the shaft speed at which natural frequency of rotor bearing system is excited and system vibration increases drastically. At critical speeds response to imbalance is maximum. Undamped critical speed analysis of rotor bearing system calculates where critical speeds will occur. Since shaft is supported by ball bearings undamped critical speed analysis was carried out. From the undamped critical speed map it was observed that first two natural frequencies related to rigid body modes are 6757rpm and 26780rpm. The third critical speed is over 100krpm; hence the entire rotor is operated at rigid body mode over all test speed range.

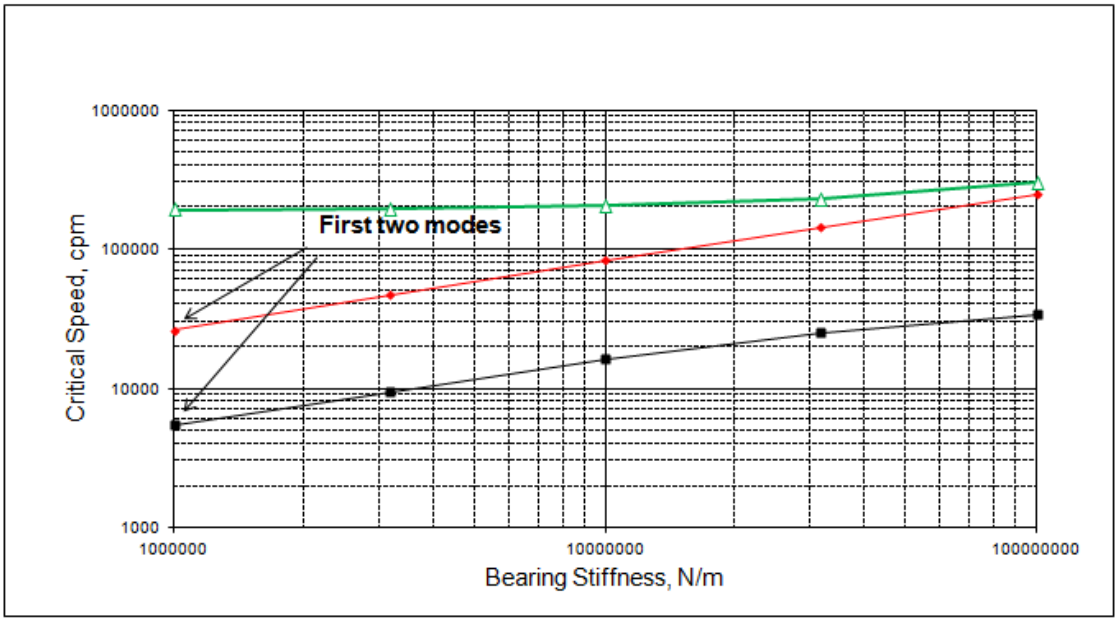

Figure 4-5 Undamped critical speed map

4.1.2 Pedestal Assembly with Rolling Element Bearings

The pedestal (Figure 4-6(a)) is the housing for the ball bearings supporting the shaft. Both ends were flanged for the ease of assembly/disassembly. All the ball bearings in the system (motor and shaft support) used Alemite 3920 oil mist lubricator. The pedestal was provided with an oil mist inlet and drain as shown Figure 4-7 to circulate lubricant through the ball bearings. The flange configuration was necessary for assembly and disassembly without any physical damage to the ball bearings. The exploded view shown in Figure 4-6(b) clears the picture of all the mating parts including the end seals.

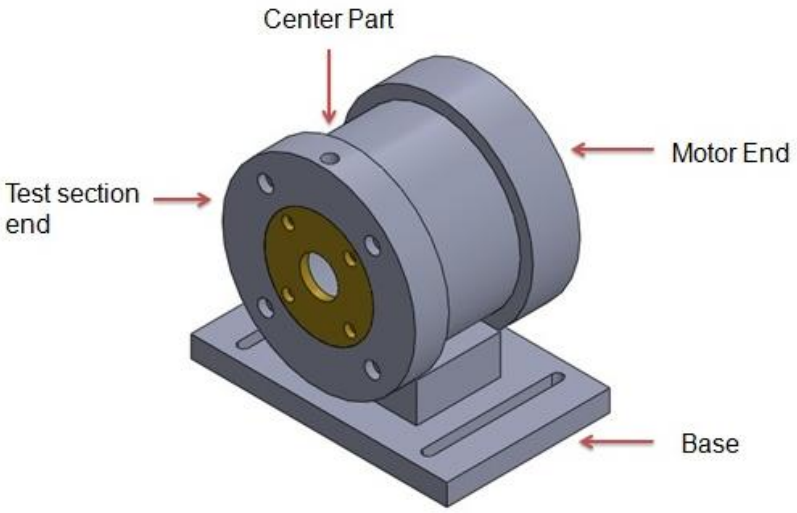

(a) CAD model of pedestal

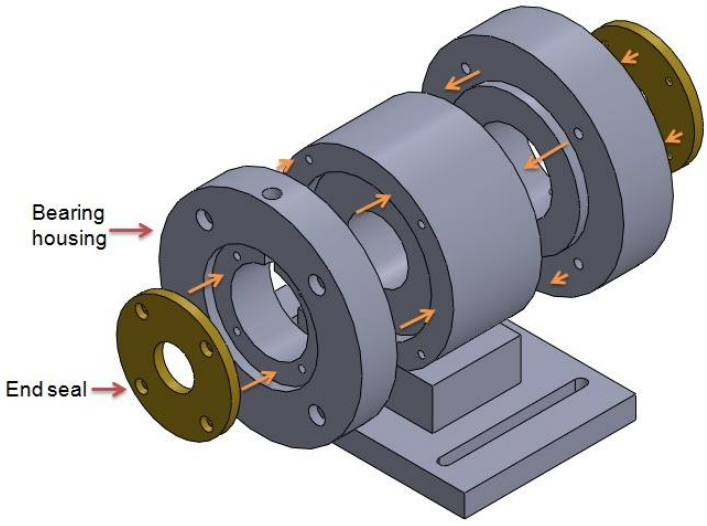

(b) Exploded view of pedestal housing

Figure 4-6 Detailed views of pedestal housing (a) Assembled cad model of pedestal (b) Exploded view of pedestal housing

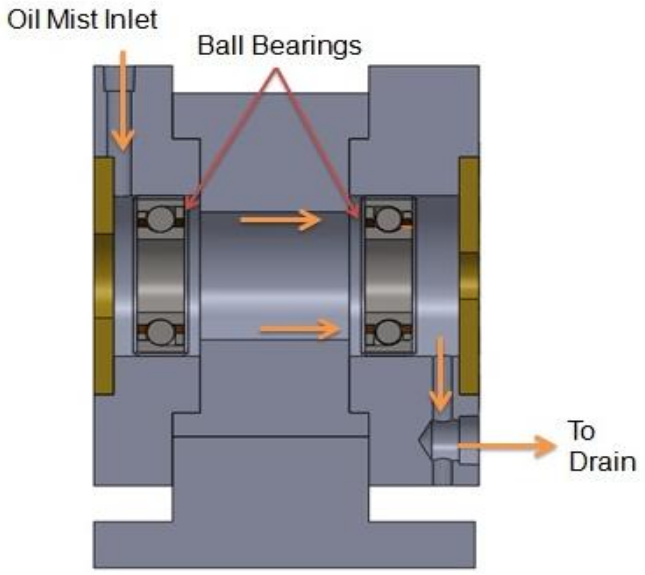

Figure 4-7 Section view showing inlet and drain of lubricant

Final assembly of pedestal housing including the main shaft is shown in Figure 4-13. The bearing is mounted in to the housing surrounded by a tolerance ring which accommodates for slight misalignment between bearings. The bearing housing also has O-rings for additional damping. To monitor the ball bearing temperature thermocouples were attached directly to the tolerance ring.

The simplest technique to assemble pedestal is,

1. First mount both the ball bearings into their respective housings taking into account the preload directions as shown in Figure 4-8.

2. Then assemble the test side end on to the shaft through the hand press as Figure 4-9

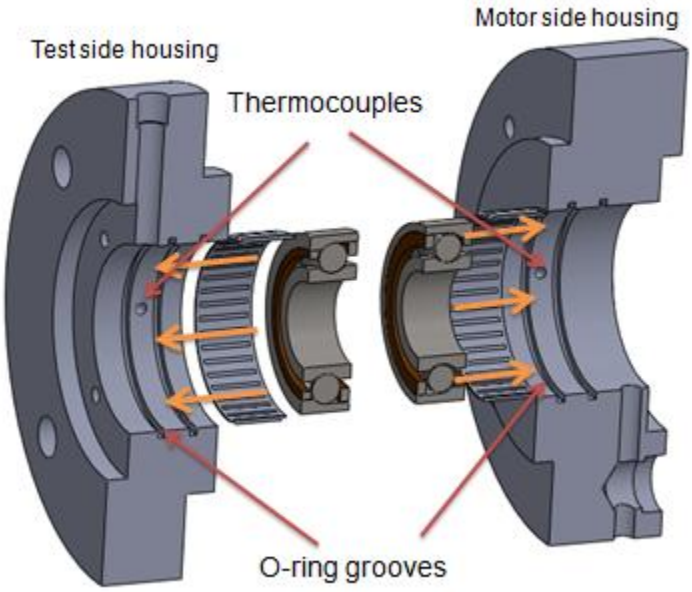

Figure 4-8 Installation of ball bearings into housing

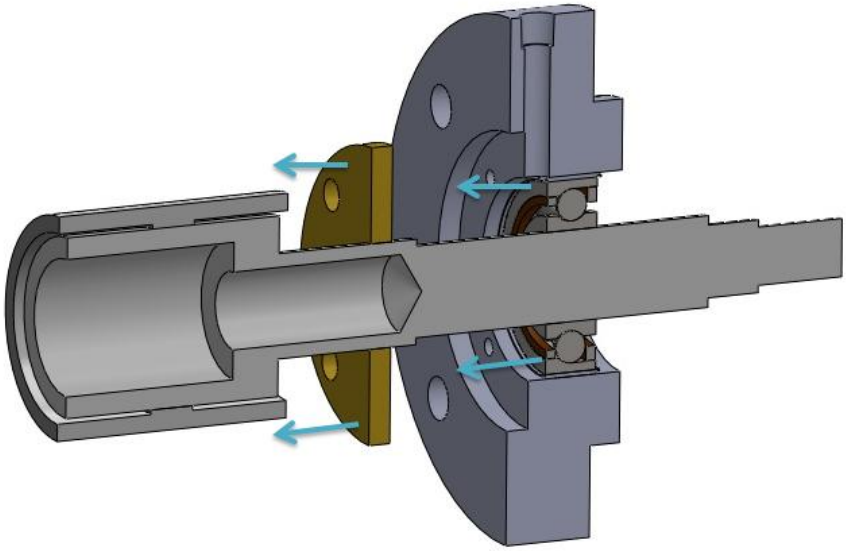

Figure 4-9 Test side housing installation

3. Once the test side housing is assembled, slowly slide the shaft into the center piece. Then mount motor side on to the shaft again using the hand press. Tighten bearing locknut and finally the end seals.

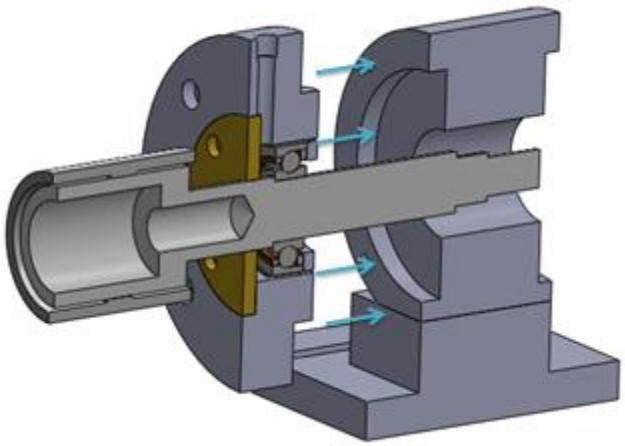

Figure 4-10 Test section mounted on center housing

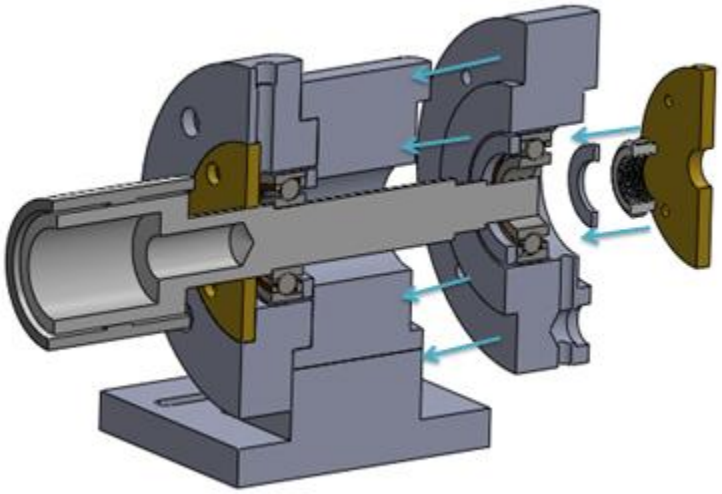

Figure 4-11 Motor side housing assembly

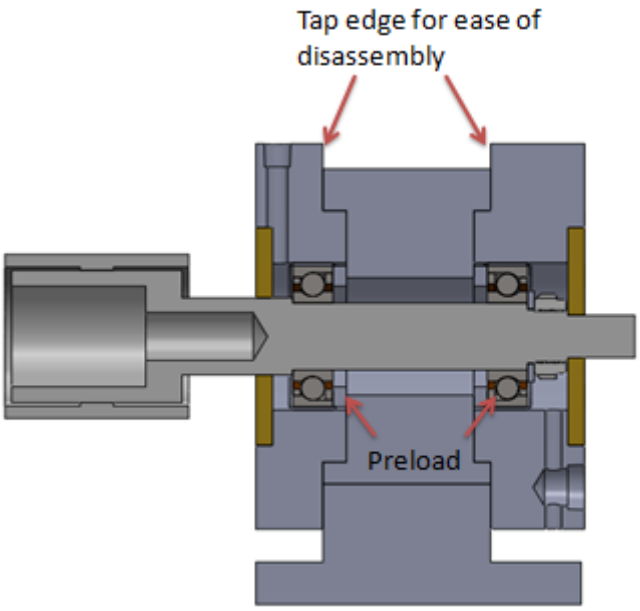

Figure 4-12 Flange configuration for ease of disassembly

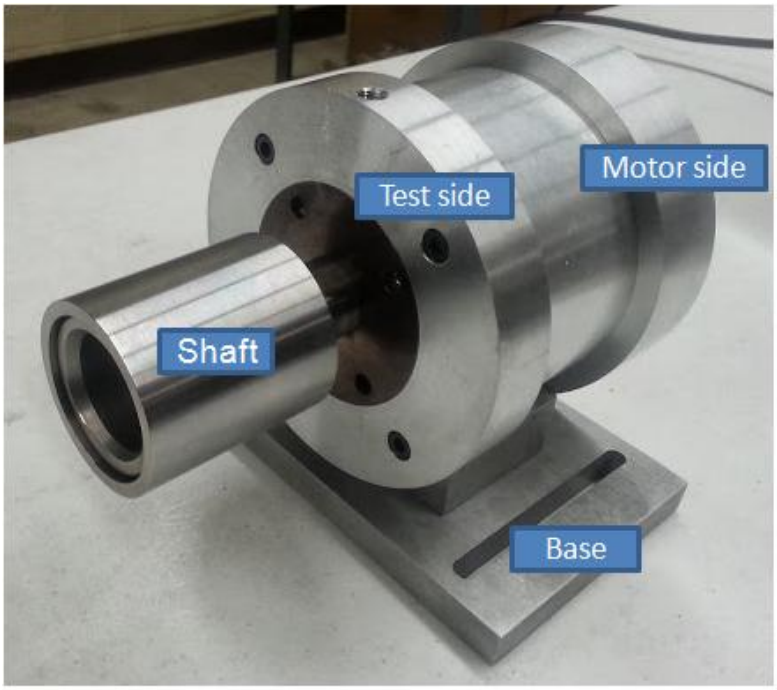

Figure 4-13 Final pedestal-shaft assembly

4.1.3 Test Section Bearing

The test bearing is a hydro-dynamically preloaded three pad air foil bearing. The bearing is housed in a split stainless steel holder for the ease of assembly and disassembly. Major components of the bearing are bearings sleeve, top foils, bumps foils. The split housing has a split end cap to direct flow through the bearing.

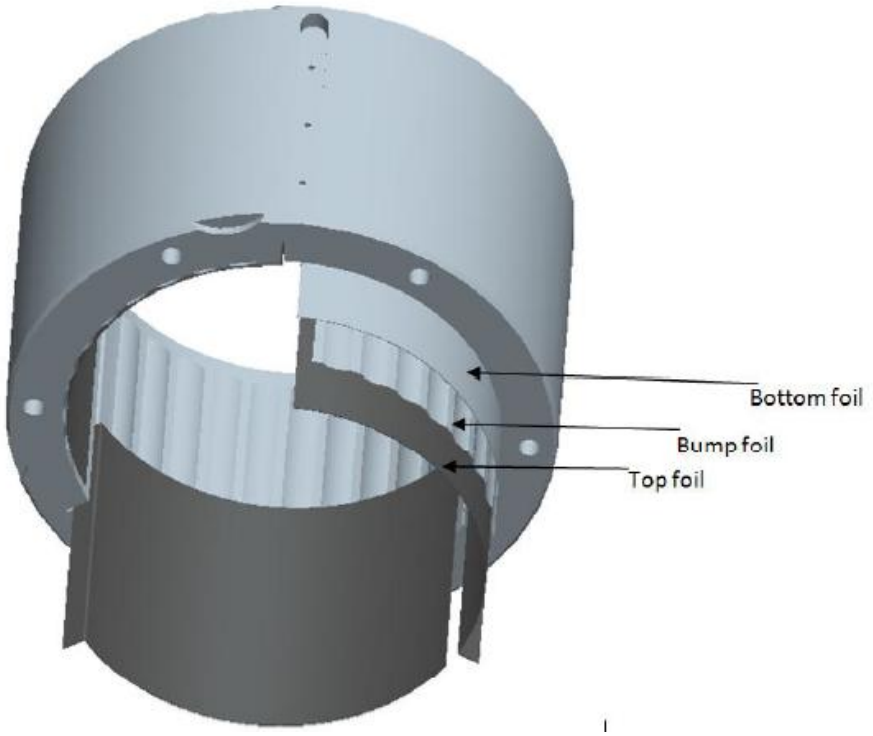

Figure 4-14 Components of bearing, adopted from ref [11]

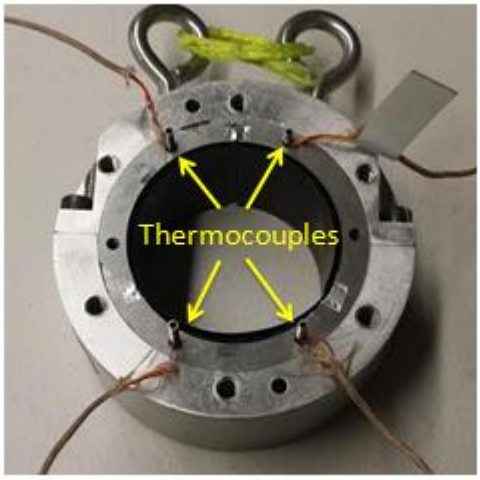

Figure 4-15 Actual bearing with thermocouple locations

Table 4-2 Bearing Specifications (unit: mm)

Rotor radius	24.5
Bearing length	37.5
Bearing radius	24.585
Top foil thickness	0.127
Bump foil thickness	0.127
Bump height	0.49
Nominal clearance(C)	0.120
Set Bore clearance(CS)	0.085

a. Bearing sleeve: Age hardened Inconel 718 was used to manufacture the sleeve. The sleeve holds top foils and bump foils in position through slots cut

along the axis. Slots are cut using electronic discharge machine. Holes on side wall were used to insert thermocouples to monitor the bearing thermal behavior shown in Figure 4-15.

b. Bump foils: Bumps provide the required stiffness and damping to bearing. Moreover, cooling channels formed in corrugated structure are supplied with cooling air to maintain the temperature of entire bearing. Three bump foils are spot welded to sleeve with bottom foils in between (see Figure 4-14). Fabrication of bump foil involves 1. Cutting rectangular blanks (50 mm x 35.5 mm) of 125 micron thick Inconel X750. 2. Using a hydraulic press for formation of bumps using a forming jig. 3. Rolling around a mandrel on diameter 1.5” to get required curvature. Since bump height is a crucial property the rolling requires special care. Finally foils are heat treated.

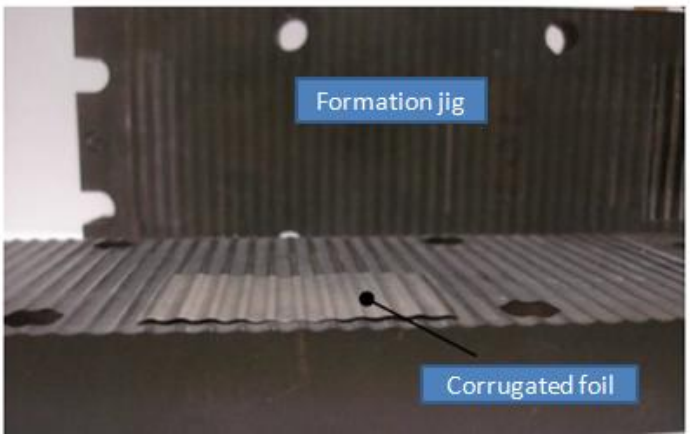

(a)

(b)

(c)

Figure 4-16 (a) Formation of Bumps (b) Rolling for curvature (c) Completed bump foil

c. Top foils: Top foil is supported by bump foil, and three separate top foils were used as shown in Figure 4-14. Top foil should have a uniform curvature as it is actual bearing surface. Lip area enters axial slot of the sleeve and holds top foil in position. Formation of top foil involves 1. Cutting rectangular blanks (52.5 mm x 37.5 mm) of 125 micron thick Inconel X750. 2. The blank is pressed in lip forming jig. 3. Once lip is formed, foil is curved using a curvature jig and finally heat treated in a furnace as shown in Figure 4-17. To reduce start/stop frictional power loss, top foil is coated with a solid lubricant Teflon.

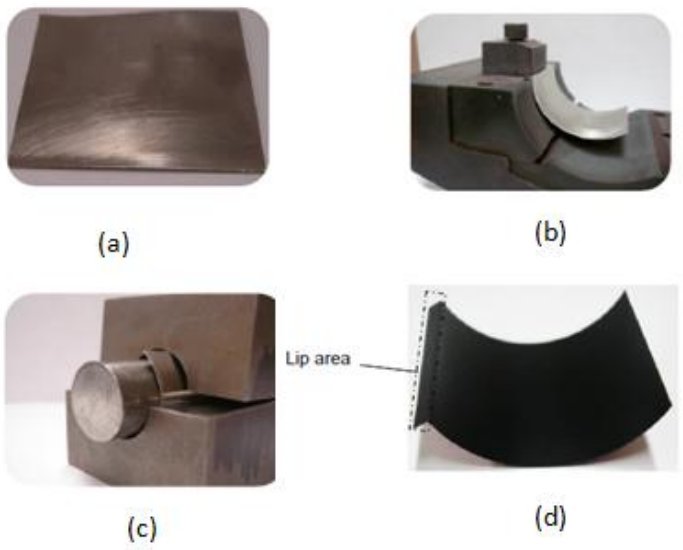

Figure 4-17 Top foil formation (a) Inconel Blank (b) Lip forming jig (c) Curvature forming jig (d)Coated top foil

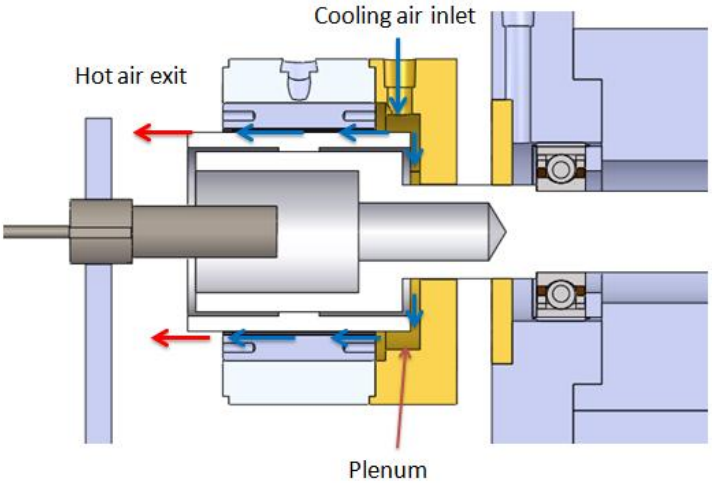

Figure 4-18 Direction of cooling air flow

4.2 Hardware

Experimental hardware includes heating mechanism, loading mechanisms, lubrication system and data acquisition systems.

4.2.1 Heating Mechanism

To mimic the actual turbine environment two high temperature heating coil cartridges (Figure 4-19) were utilized. These single phase heaters have magnesium oxide insulation and Incoloy sheath housing. The heaters employed a controller which could provide the required voltage to reach the desired temperatures. The heater can withstand a temperature of 870^{o}C.

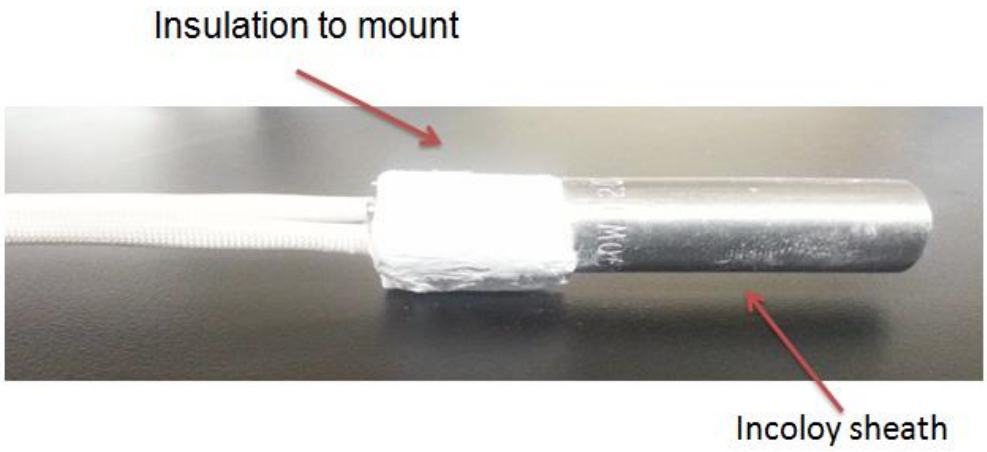

Figure 4-19 Cartridge heater

4.2.2 Air Heater

A simple air heater was made to provide cooling air to the test bearing. The cooling air supplied was heated up to 90^{o}C. A 6" cartridge heater was incorporated in a tubing to increase the cooling air temperature.

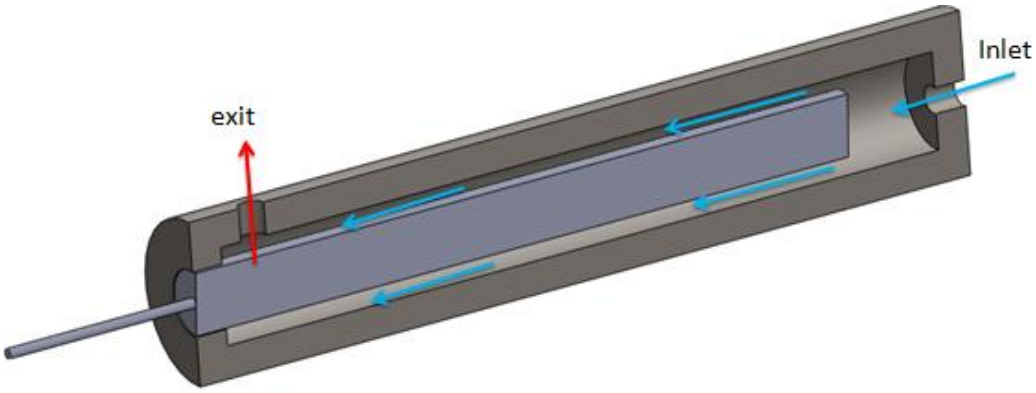

Figure 4-20 Air heater used to supply hot air to test bearing

4.2.3 Data Acquisition System

The experimental data was collected through National Instruments Labview VI's, the instrumentation included pressure transducer, thermocouples and load cell.

a. Pressure transducer: Air pressure at the inlet was monitored using a pressure transducer (PX409-2.5G5V) from Omega, Inc, maximum capacity of 2.5 psig. A 10V power supply was employed to power the device and output voltage from the sensor was fed to the NI chassis through NI9205 input module. The chassis was connected to computer which used a Labview VI that processed voltage to pressure reading.

b. Torque measuring mechanism: Torque measurement helps in monitoring friction during operation. A 120 mm long torque rod was attached to bearing housing that transmitted bearing friction load to PCB load cell. The load cell transferred the voltage to Labview VI which processed the voltage reading to torque signal.

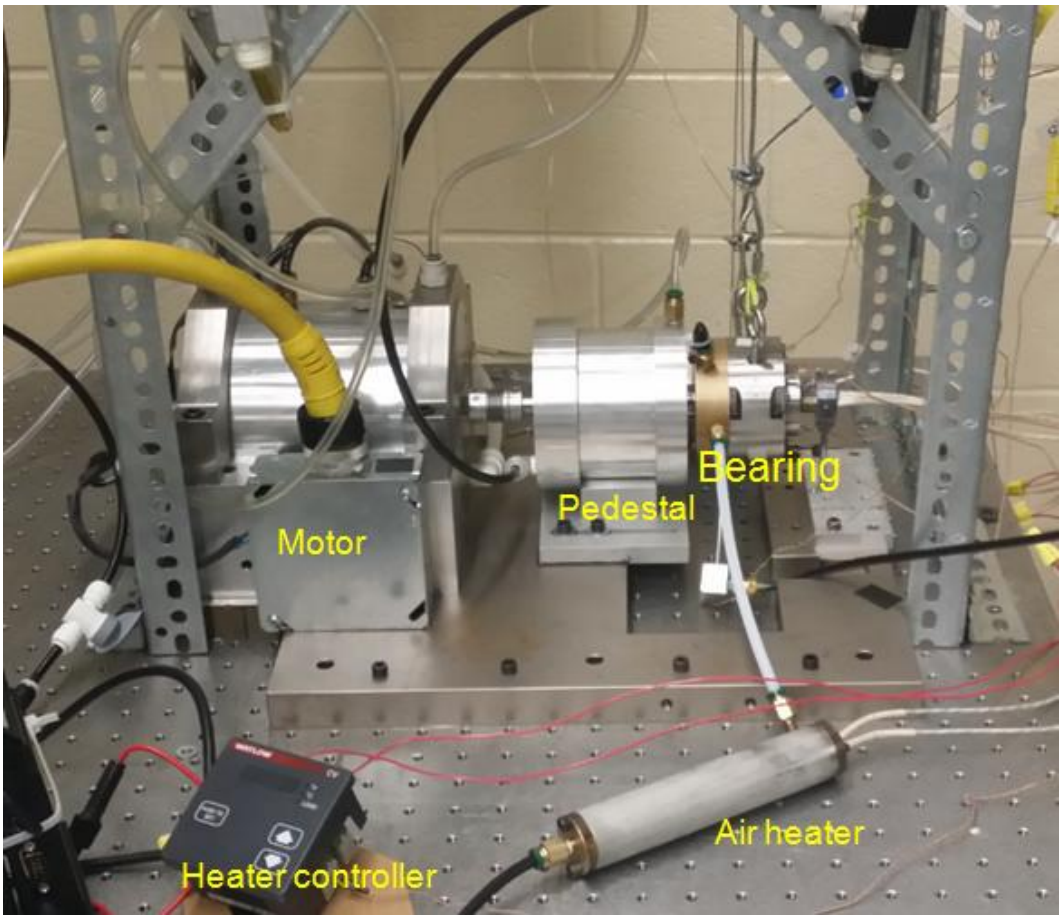

Figure 4-21 Photo of high temperature test rig

c. Temperature measurement: Thermocouples were used to measure temperature of bearing housing, bearing sleeve, heating coils and ball bearing housing.

One issue was found during the experiments: Insufficient interference between inner race of the ball bearing and shaft lead to sudden increase in vibration of shaft at high speeds. Due to this slip at timely intervals a sudden increase in amplitude of vibration was observed, this vibration transferred to the test bearing and generating large fluctuation on the load cell in the torque measurement mechanism. This jumping behavior of rig was minimized by increasing the shaft temperature by preheating the setup before actual experiment, until sufficient thermal interference between shaft and inner race was achieved.

.

Chapter 5

Results and Discussion

The thermal distribution on the length of the shaft was evaluated by heating the test rig at cartridge temperature of 400 and 600^{o}C at stationary condition. Temperature was measured at outer and inner edge of both main shaft and journal shaft. Thermal gradient on the main shaft in the axial direction was observed to be around 60^{o}C where as the thermal gradient on the journal shaft was 10^{o}C for both the conditions.

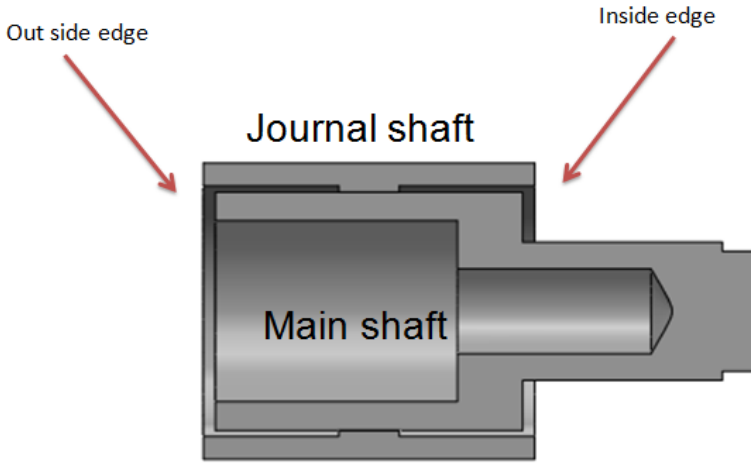

Figure 5-1 Thermocouple locations to measure temperature in a stationary shaft

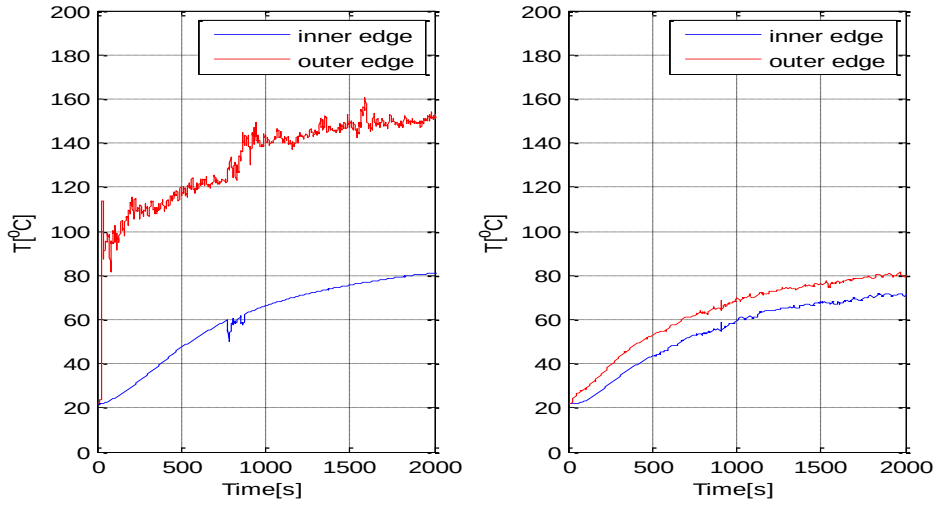

(a) (b)

Figure 5-2 Temperature of shaft in test section at 400°C in stationary condition

(a) Thermal gradient on main shaft (b) Thermal gradient on journal

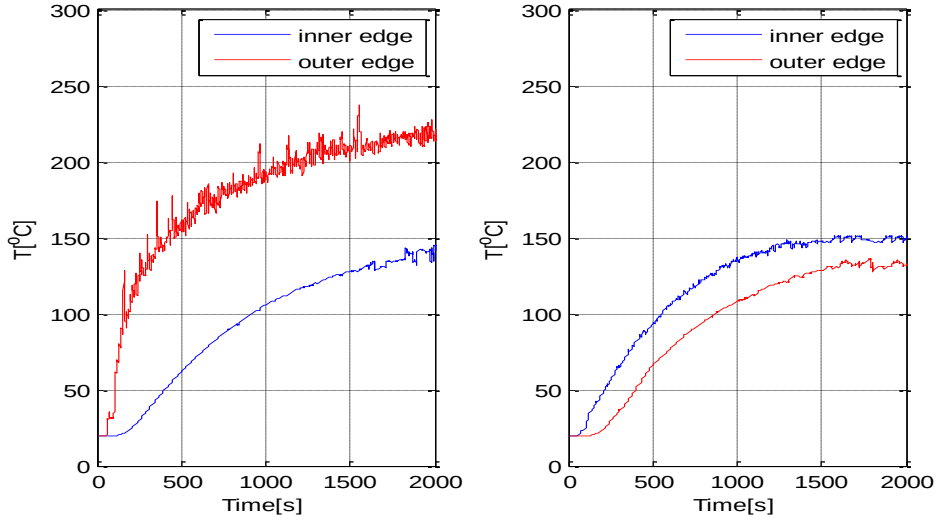

(a) (b)

Figure 5-3 Temperature of shaft in test section at 600°C in stationary condition (a)

Thermal gradient on main shaft (b) Thermal gradient on journal

Tests were carried out at 15-25krpm by heating the test section between cartridge temperature 600^{o}C to 800^{o}C with a constant pressure drop of 800 Pascal. A static load of 45N was applied to the test bearing throughout the tests.

The temperature of the bearing was monitored at four different locations along the circumference. The overall bearing temperature during normal operation is shown in Figure 5-5

The bearing holder was exposed to environment, and the holder temperature was substantially less than other bearing components due to convection to ambient air. The temperature evolution until steady state is shown in Figure 5-4.

Thermocouple was inserted into the cooling jacket to measure the temperature of the cooling air inlet plenum. Figure 5-6 shows the temperature in the bearing plenums for all the cases.

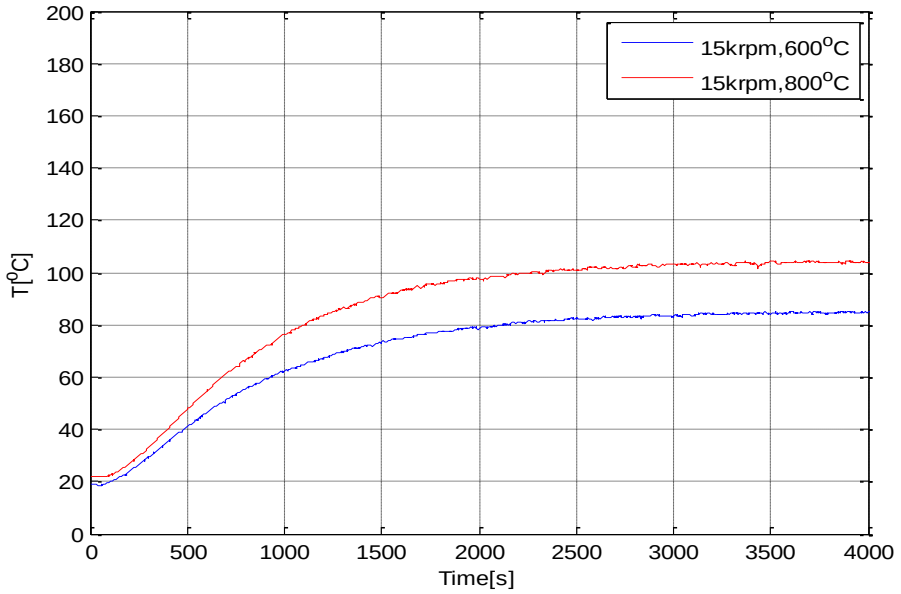

(a)

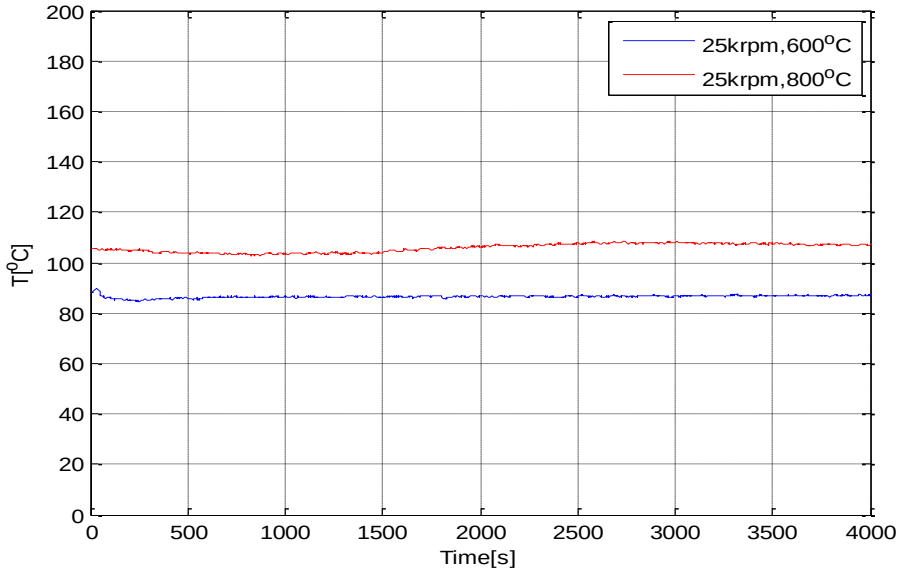

(b)

Figure 5-4 Temperature evolution of bearing holder at (a) 15krpm (600°C-800°C)

(b) 25krpm (600°C-800°C)

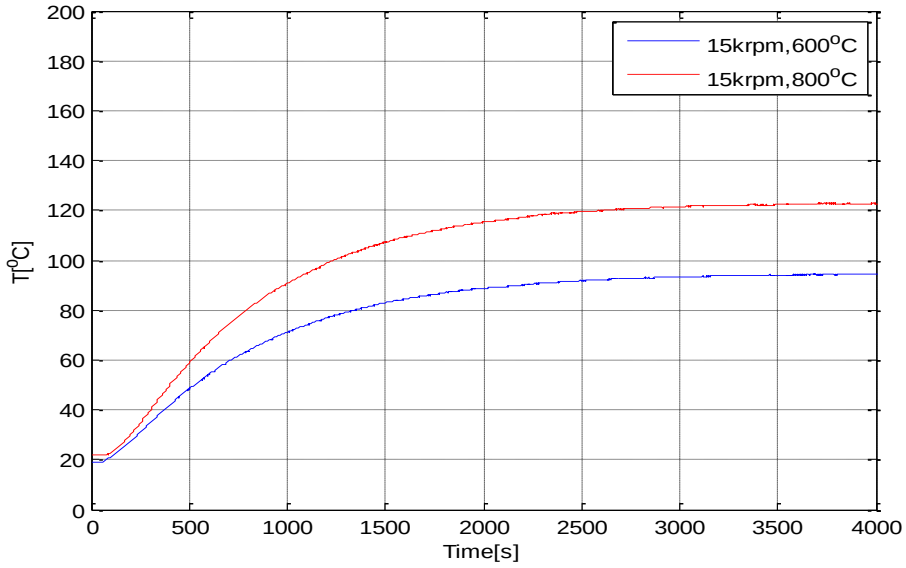

(a)

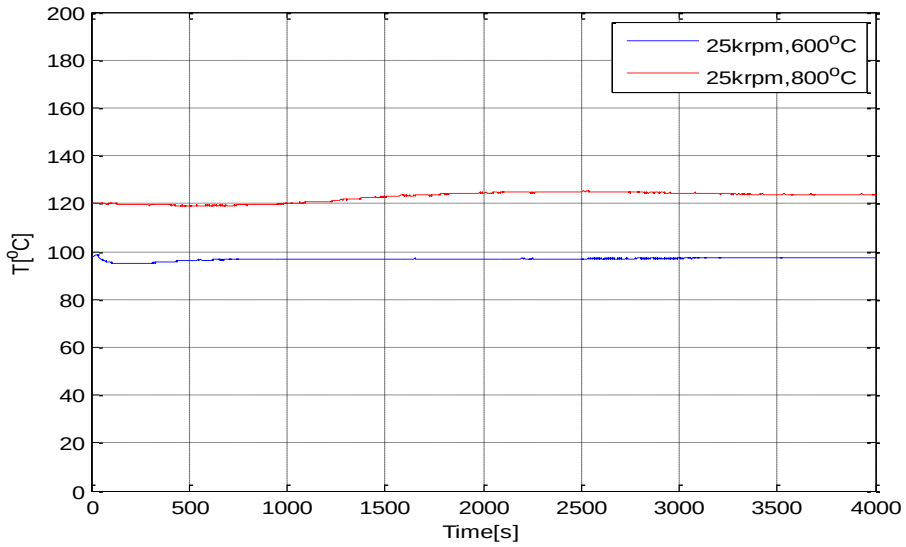

(b)

Figure 5-5 Temperature evolution of three-pad foil bearing at (a) 15krpm (600°C-800°C) (b) 15krpm (600°C-800°C)

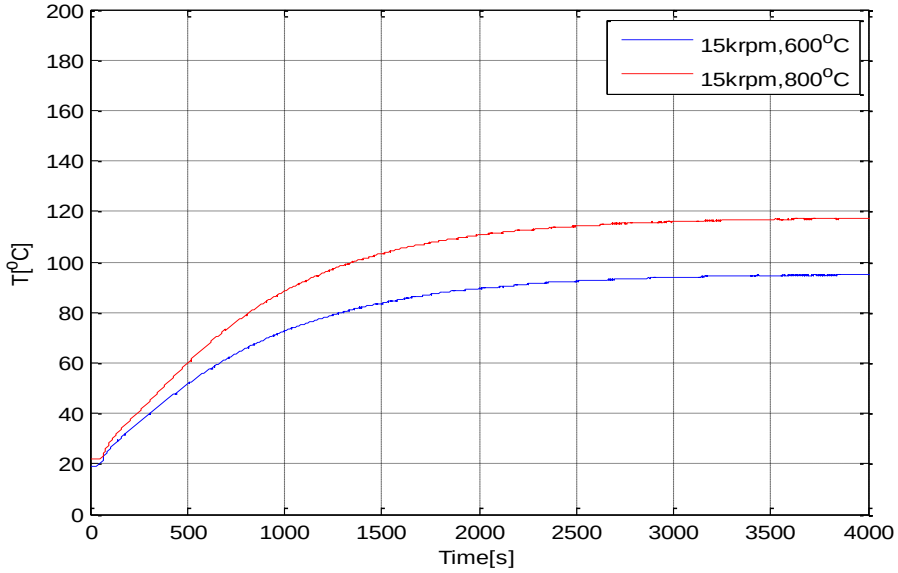

(a)

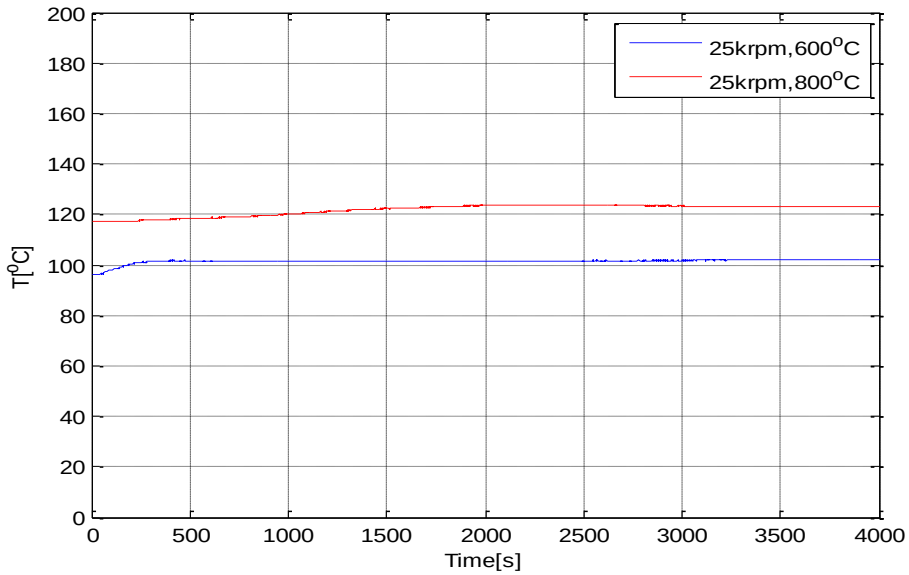

(b)

Figure 5-6 Temperature evolution of plenum at (a) 15krpm (600°C-800°C) (b) 25krpm (600°C-800°C)

Chapter 6

Conclusion and Future Work

6.1 Conclusion

The high temperature test rig to mimic turbine hot section was functional up to 25,000 rpm within a cartridge temperature of 800^{o}C. A steady operating condition was achieved using the three pad foil bearing. Further, reduction in heat transfer through conduction was achieved from the main shaft to the journal shaft, also thermal gradient along the length on journal shaft was observed to be substantially lower than main shaft.

6.2 Future Work

The future work on this test rig may include modification of the shaft to increase speed. The main shaft diameter where rolling element bearings are assembled has to be increased to have slight interference fit with the inner race of the ball bearing. Increasing the diameter (approximately by 0.02mm) of the shaft in the support region might solve this issue. Also the concentricity between the journal and main shaft needs to be improved by providing tighter manufacturing tolerances.

Even if heater temperature is 800^{o}C, main shaft temperature is only 250^{o}C because there is not much interacting area between the heater and main shaft. Using a longer main shaft and higher capacity cartridge heater might improve heat transfer from heater to the main shaft. Figure 6-1, shows the suggested improvement with longer main shaft.

Controlling the thermal boundary condition of bearing holder (currently convection ambient air) using a band heater around it will allow more realistic turbine hot section environment.

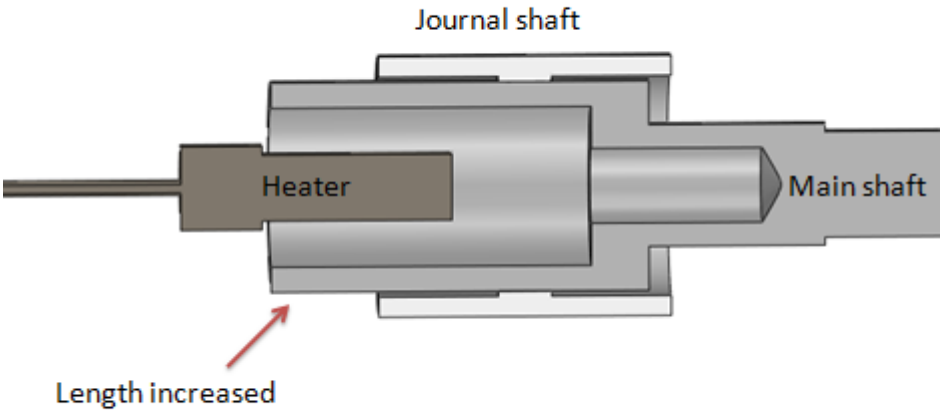

Figure 6-1 Longer main shaft to increase interacting area with cartridge heater

Appendix A

Test rig in operation at 25krpm and cartridge heater temperature 800^{o}C

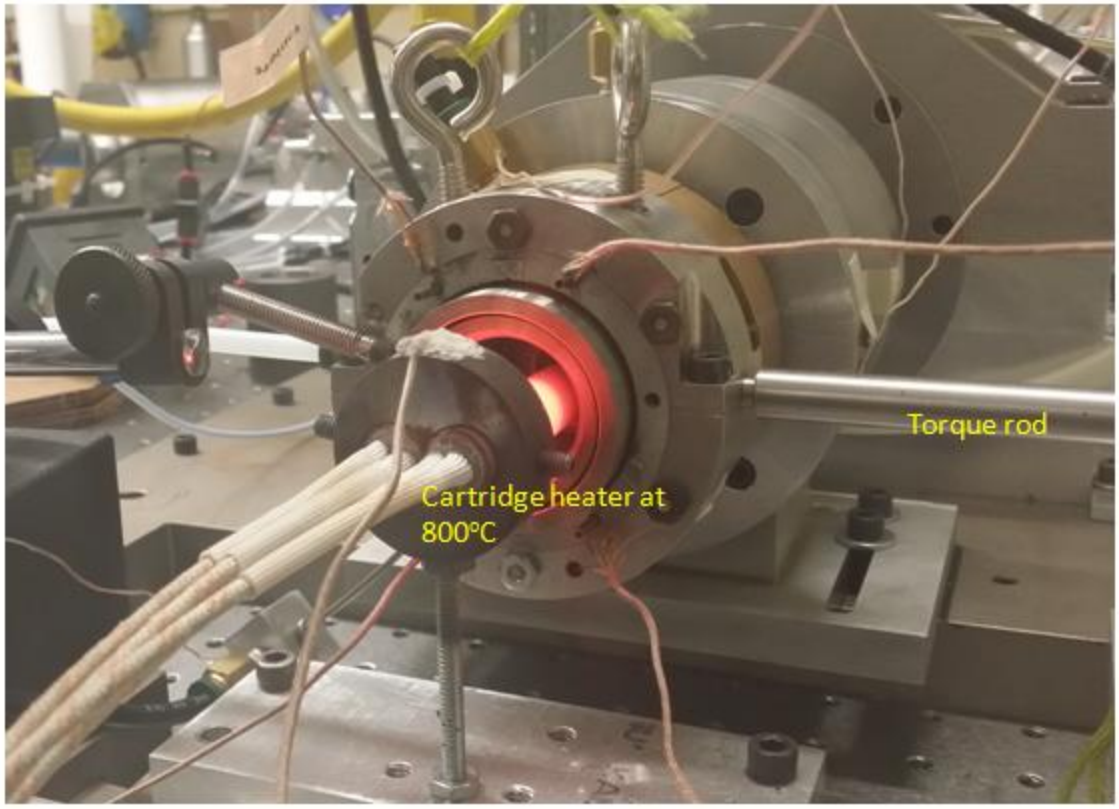

Figure A-0-1 Test rig in operation at 25krpm and cartridge heater temperature 800^{o}C

Bibliography

[1] Lee, D., and Kim, D., 2010, "Thermo-Hydrodynamic Analyses of Bump Air Foil Bearings with Detailed Thermal Model of Foil Structures and Rotor," ASME Journal of Tribology**, 132**(2), pp. 021704 (12 pages).

[2] Kim, D., 2007, "Parametric Studies on Static and Dynamic Performance of Air Foil Bearings with Different Top Foil Geometries and Bump Stiffness Distributions," ASME Journal of Tribology**, 129**(2), pp. 354-364.

[3] Salei, M., Swanson, E., and Heshmat, H., 2001, "Thermal Features of Compliant Foil Bearings – Theory and Experiments," ASME Journal of Tribology**, 123**(3), pp. 566-571.

[4] Radil, K., Howard, S., and Dykas, B., 2002, "The Role of Radial Clearance on the Performance of Foil Air Bearings," STLE Tribology Transaction**, 45**(4), pp. 485-490.

[5] Radil, K., and Zeszotek, M., 2004, "An Experimental Investigation into the Temperature Profile of a Compliant Foil Air Bearing," STLE Tribology Transactions**, 47**(4), pp. 470-479.

[6] Dykas, B., and Howard, S. A., 2004, "Journal Design Considerations for Turbomachine Shafts Supported on Foil Air Bearings," STLE Tribology Transactions**, 47**(3), pp. 508-516.

[7] Radil, K., DellaCorte, C., and Zeszotek, M., 2007, "Thermal Management Techniques for Oil-Free Turbomachinery Systems," STLE Tribology Transactions**, 63**(10), pp. 319-327.

[8] Kim T, Breedlove AW, and San Andrés L., 2009, "Characterization of a Foil Bearing Structure at Increasing Temperatures: Static Load and Dynamic Force Performance." Journal of Tribology**, 131**(4), pp. 041703-041703-9.

[9] Radil, K., and Batcho, Z., 2010, "A Novel Thermal Management Approach for Radial Foil Air Bearings," **, DTIC Document**.

[10] Kim, D. J., Ki, J. P., Kim, Y. C., and Ahn, K. Y., 2012, "Extended Three-Dimensional Thermo-Hydrodynamic Model of Radial Foil Bearing," Journal of Engineering for Gas Turbines and Power**, 134**(5), pp. 052501.

[11] Shrestha SK, Kim D, Cheol Kim Y., 2013, "Experimental Feasibility Study of Radial Injection Cooling of Three-Pad Air Foil Bearings." J. Tribol..**, 135(4)**, pp. 041703-041703-9.

[12] Kim, D., Lee, D., Kim, Y. C., and Ahn, K. Y., 2010, "Comparison of Thermo-Hydrodynamic Characteristics of Airfoil Bearings with Different Top Foil Geometries," Proceedings of the 8th IFToMM International Conference on Rotordynamics, Seoul, Korea, September 12-15, Paper No. WeD1-4.

Biographical Information

Tejas Devidas Patil completed his Master of Science degree in Mechanical Engineering at The University of Texas at Arlington, USA. He completed his Bachelors of Science in Mechanical Engineering from Mumbai University, India. He joined Micro turbo-machinery and Energy system laboratory under Dr. Daejong Kim in fall 2012. His research interest includes Thermal management of foil bearing in turbine hot section which is the topic of his thesis.